Bifunctional Reagents for Formylglycine Conjugation: Pitfalls and Breakthroughs

Nils Janson,[a] Tobias Krüger,[a] Lennard Karsten,[b] Mareile Boschanski,[c] Thomas Dierks[+],*[c] Kristian M. Müller,*[b] and Norbert Sewald*[a]

Dedicated to the memory of Thomas Dierks

Formylglycine-generating enzymes specifically oxidize cysteine within the consensus sequence CxPxR to C^{α}-formylglycine (FGly). This noncanonical electrophilic amino acid can subsequently be addressed selectively by bioorthogonal hydrazino-*iso*-Pictet-Spengler (HIPS) or Knoevenagel ligation to attach payloads like fluorophores or drugs to proteins to obtain a defined payload-to-protein ratio. However, the disadvantages of these conjugation techniques include the need for a large excess of conjugation building block, comparably low reaction rates and limited stability of FGly-containing proteins. Therefore, functionalized clickable HIPS and *tandem* Knoevenagel building blocks were synthesized, conjugated to small proteins (DARPins) and subsequently linked to strained alkyne-containing payloads for protein labeling. This procedure allowed the selective bioconjugation of one or two DBCO-carrying payloads with nearly stoichiometric amounts at low concentrations. Furthermore, an azide-modified *tandem* Knoevenagel building block enabled the synthesis of branched PEG linkers and the conjugation of two fluorophores, resulting in an improved signal-to-noise ratio in live-cell fluorescence-imaging experiments targeting the EGF receptor.

Introduction

In recent years site-specific bioconjugation chemistry has been used as a powerful tool to modify proteins and study their biological function.[1–4] Furthermore, it enables selective protein fusion, enzyme immobilization or the production of antibody–drug conjugates (ADC).[5–8] In order to retain the protein functions, these methods are to be biocompatible, highly selective, fast and noninvasive for living cells.

Noncanonical amino acids like *p*-azidophenylalanine can be introduced via complex genetic engineering of living cells and an expanded genetic code.[9,10] Alternatively, enzymatic modifications with short amino acid sequences, as catalyzed by sortase,[11–13] transglutaminase[14–17] or protein farnesyl transferase,[18] can be used to avoid these complex manipulations. Additionally, unique electrophilic aldehyde moieties can be introduced into proteins. On one hand, an *N*-terminal α-oxo aldehyde can be obtained by oxidation of serine or threonine[19] or by a transamination reaction of *N*-terminal glycine with pyridoxal-5′-phosphate (PLP).[20] On the other hand, the oxygen- and copper-dependent formylglycine-generating enzyme (FGE) can be used. It catalyzes the site-specific oxidation of cysteine within the consensus sequence CxPxR (aldehyde tag) to form the noncanonical amino acid C^{α}-formylglycine (FGly).[21–28] This enzyme has already been used for efficient in vitro and in vivo FGly formation.[6–8,28] Compared to the α-oxo aldehyde, which can only be generated *N*-terminally, the aldehyde tag can be inserted at almost any desired location within recombinant proteins.

Several aldehyde-specific reactions with strong nucleophiles were developed in the past. First attempts used hydroxylamines and hydrazines, which form oximes or hydrazones under acidic conditions, but are sensitive to hydrolysis.[29–36] Further research resulted in the development of the (hydrazino-*iso*-)Pictet-Spengler (HIPS) reaction using modified tryptamines that undergo a Mannich-type reaction with respective aldehydes. After proton-catalyzed condensation (pH 5.5–6.5), the iminium ion formed is converted by an intramolecular nucleophilic attack of the indole moiety.[37–39] Moreover, Pomplun et al. reported a similar reaction using *N*-substituted pyrrolyl alanine derivatives.[40]

[a] *N. Janson, Dr. T. Krüger, Prof. N. Sewald*
Faculty of Chemistry, Organic and Bioorganic Chemistry
Bielefeld University
Universitätsstraße 25, 33615 Bielefeld (Germany)
E-mail: norbert.sewald@uni-bielefeld.de
[b] *L. Karsten, Prof. Dr. K. M. Müller*
Cellular and Molecular Biotechnology
Bielefeld University
Universitätsstraße 25, 33615 Bielefeld (Germany)
E-mail: kristian.mueller@uni-bielefeld.de
[c] *M. Boschanski, Prof. Dr. T. Dierks[+]*
Faculty of Chemistry, Biochemistry
Bielefeld University
Universitätsstraße 25, 33615 Bielefeld (Germany)
[+] *Thomas Dierks passed away on July 07, 2020*

Supporting information for this article is available on the WWW under https://doi.org/10.1002/cbic.202000416

This article is part of a joint Special Collection with the Journal of Peptide Science on SPP 1623: Chemoselective reactions for the synthesis and application of functional proteins. Please see our homepage for more articles in the collection.

Alternatively, carbon nucleophiles may be used for aldehyde-labeling, like in Wittig,[41] Mukaiyama aldol[42] and aldol reactions with 2,4-thiazolidinediones[43] or *N*-aliphatic substituted pyrazolones. In the latter case, a double bond is formed at neutral pH, which can either be attacked by an intramolecular thiol (*trapped* Knoevenagel)[8] or a second pyrazolone building block (*tandem* Knoevenagel).[44] *N*-aryl substitution of those moieties further increases reactivity.[45] HIPS and Knoevenagel ligation have already been used in combination with the aldehyde-tag to produce site-specific ADCs with defined drug-to-antibody ratios (DAR). However, a large excess of the expensive drug-containing building block and long reaction times were necessary.[7,8,44]

To avoid these aforementioned disadvantages, we have established an efficient and straightforward synthesis of inexpensive bifunctionalized HIPS and *tandem* Knoevenagel building blocks, which can be used in combination with highly efficient strain-promoted azide alkyne cycloadditions (SPAAC) for selective mono- or double-derivatization with stoichiometric amounts of DBCO-modified payloads (Scheme 1).

Results and Discussion

Synthesis of HIPS and Knoevenagel conjugation reagents

In order to address formylglycine residues with modular HIPS and Knoevenagel ligation reagents combined with either strain-promoted azide alkyne cycloadditions (SPAAC) or inverse electron-demand Diels-Alder reaction (IEDDA), we synthesized an array of bio-orthogonally reactive HIPS and Knoevenagel building blocks.

The Fmoc protected hydrazine **1** (Scheme 2A) and the pyrazolone-type Knoevenagel core segments **8** and **11** (Scheme 3A and B) were synthesized similar to literature protocols.[7–8,28,44–45] Subsequently, bifunctionalized HIPS ligation reagents were obtained containing the *N*,*N*′-dimethylhydrazine group for FGly conjugation together with an azide, a bicyclononyne (BCN), a dibenzocyclooctyne (DBCO) or a 6-methyltetrazine (mTet) moiety for SPAAC or iEDDA, respectively. Amide couplings were accomplished using DCC/EDC and pentafluorophenol/HOBt to form the corresponding PFP or HOBt ester,[28] which reacts with amine functionalized azide-, BCN-, DBCO- or 6-methyl-tetrazine derivatives. Finally, Fmoc cleavage was performed by treatment with sodium hydroxide or 20% piperidine.

However, during the syntheses of different envisaged building blocks we encountered problems because of incompatibilities of reagents and/or functional groups. The purification of the alkyne-containing HIPS-BCN (**5**) could be performed by RP-HPLC omitting acidic additives, since we observed two major side products with mass signals at *m/z* 586.37 (Figure S8 in the Supporting Information) and *m/z* 1135.72 (Figure S9) during purification in the presence of 0.1% TFA. These signals could be related to a water adduct of the desired product (m/z_{calc} 586.36 $[M+H_2O+H]^+$) and a dimer (m/z_{calc} 1135.69), indicating acid-mediated addition of nucleophiles, like hydrazine or water, to the strained alkyne. As a result, either an enamine or an enol is formed that tautomerizes to the corresponding ketone (Scheme 2B.1). The water addition was also observed and fully characterized by Spangler et al.[46] Instead of the nucleophilic addition of the hydrazine to the vinyl cation formed upon protonation of the strained alkyne, it can also be considered that the hydrazine moiety reacts with the aforementioned formed ketone, which would lead to the same enamine side product (Scheme 2B.1).

First attempts to purify the literature known HIPS-DBCO (**4**)[47] on silica gel failed due to complete decomposition during flash chromatography. Instead, purification by RP-HPLC led to low yield encountered together with unsatisfactory purity. This

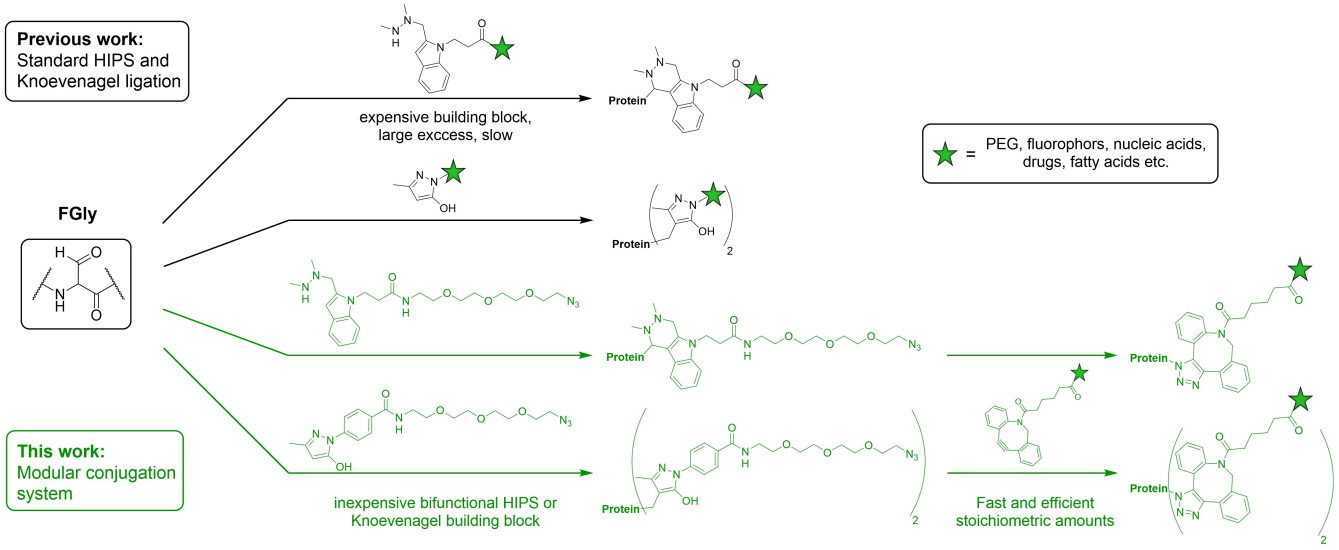

Scheme 1. Development of a highly efficient modular conjugation system for mono- and double conjugation by using stoichiometric amounts of DBCO derivatives.

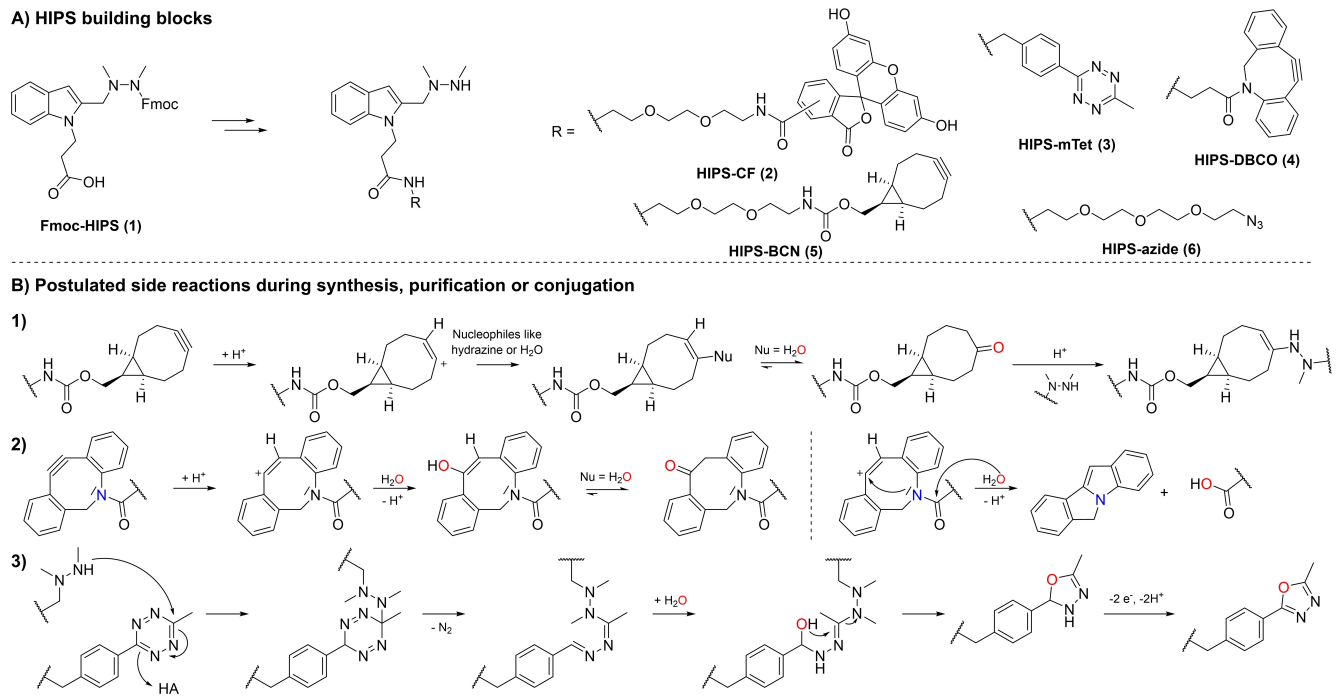

Scheme 2. Bifunctional HIPS reagents and observed side reactions. A) Two-step synthesis (coupling and deprotection) of HIPS-CF (**2**), -mTet (**3**), -DBCO (**4**), -BCN (**5**), and -azide (**6**). B) Postulated side reactions during synthesis, purification or conjugation. 1) Postulated acid-mediated decomposition of BCN. 2) Possible mechanism for proton catalyzed decomposition of DBCO. 3) Observed inter- or intramolecular hydrazine-catalyzed decomposition of HIPS-mTet (**3**).

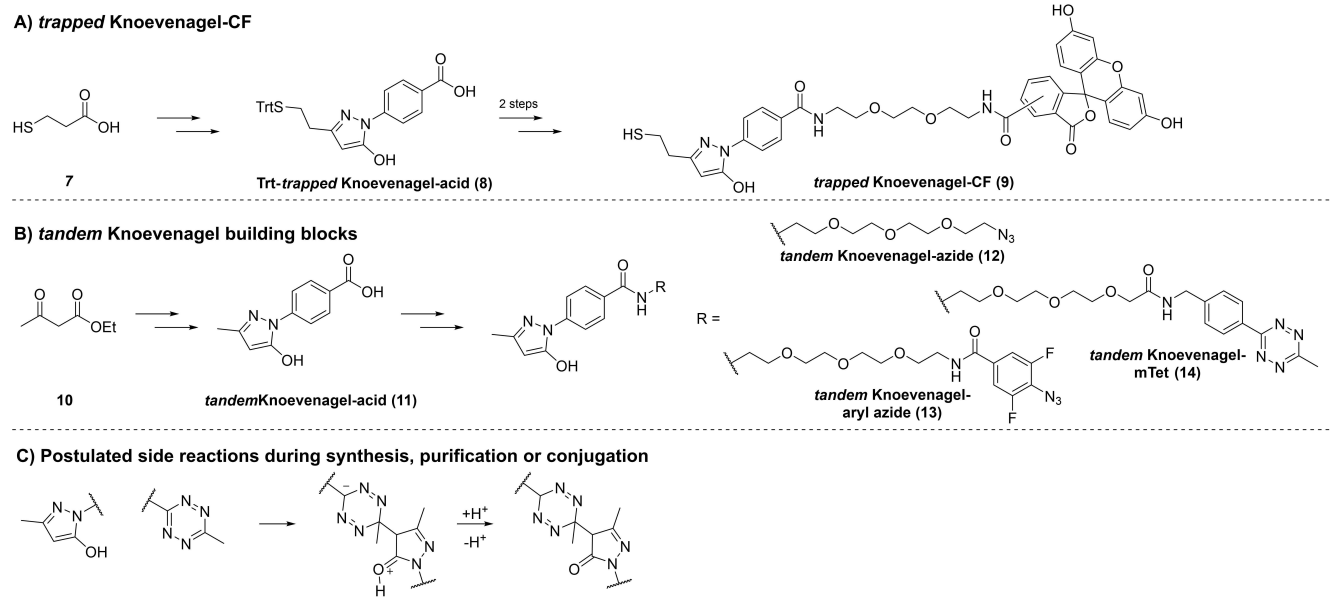

Scheme 3. Bifunctional Knoevenagel reagents and observed side reactions during synthesis, purification or conjugation. A) Synthesis of *trapped* Knoevenagel-CF (**9**) starting from 3-mercaptopropionic acid (**7**). B) Synthesis of *tandem* Knoevenagel-azide (**12**), fluorine-substituted aryl azide (**13**) and -mTet (**14**). C) Postulated inter- and intramolecular side reaction of pyrazolone with methyl substituted tetrazine.

can be explained by decomposition reactions, caused by oxidation of the hydrazine moiety, which was observed for all HIPS reagents (Figure S6). Additionally, an intramolecular attachment to the vinyl cation of the amide nitrogen accompanied by amide hydrolysis presumably forms 6*H*-isoindolo[2,1-a]indole (Scheme 2B.2 and Figure S6), which would fit to the literature known decomposition of Cbz-protected DBCO under acidic or basic conditions.[48]

Improved reactivities towards BCN or cyclooctenes have been observed for tetrazines as reaction partners.[49] However,

purification of the bifunctional building block HIPS-mTet (**3**) was not possible due to a fast decomposition upon Fmoc cleavage. LC–MS analysis of the mixture revealed a major side product with a mass shift of −22 Da that might correspond to a 5-methyl-1,3,4-oxadiazole derivative (Scheme 2B.3 and Figure S7) formed by hydrazine-catalyzed decomposition, which proceeds similarly to previously described reactions.[50–51]

As observed for **4** and **5**, purification of HIPS-azide (**6**) with RP-HPLC led to product decomposition. Interestingly, this was even observed in the absence of TFA and might have been caused due to an increase inherent susceptibility of **6** towards oxidation at the hydrazine moiety. However, **6** could be isolated in sufficient purity upon precipitation of the dibenzofulvene-piperidine side-product formed upon Fmoc cleavage by dilution of the reaction mixture with water. In contrast, no side reactions involving the azide group were observed, indicating sufficient orthogonality between both functionalities.

In summary, bifunctional HIPS reagents containing azide, BCN or DBCO could be prepared, albeit limited compatibility of the hydrazine and these functional groups was observed. An acidic environment leads to the addition of water to the strained alkynes or amide hydrolysis, complicating purification procedures. Introduction of a tetrazine group causes immediate decomposition. Therefore, HIPS building block **6**, showing sufficient stability and orthogonality of the functional groups, appeared to be the most promising candidate for following bioconjugation reactions.

Besides the HIPS conjugation reagents, a similar modular system for mono-conjugation with the *trapped* Knoevenagel building block containing an intramolecular thiol would be conceivable. However, DBCO, BCN, azides, and tetrazines had previously been shown to be incompatible with the required reaction conditions or high concentrations of thiols.[52–55]

Therefore, bifunctionalized *tandem* Knoevenagel ligation reagents with a pyrazolone for FGly conjugation and an alkyl azide (**12**), an aryl azide (**13**), or a tetrazine (**14**) were synthesized in moderate to good yields and in excellent purities (Scheme 3B). A mixture of tautomers was obtained in each case with varying hydroxypyrazole/4*H*-pyrazolone ratios depending on solvent and pH (Figures S1 and S2). DBCO and BCN had to be avoided because of decomposition (*vide supra*). Purification of **14** was particularly challenging because of a rapid inter- or/and intramolecular attack of the pyrazolone moiety to the electrophilic methyltetrazine (Scheme 3C), slowly leading to a cyclization at low concentrations (1 mM; Figure S5). However, at higher concentrations cyclization as well as a dimerization of two molecules of **14** was observed (Figure S4). Interestingly, in contrast to previous observations[56] and the hydrazine-catalyzed decomposition of **3**, no nitrogen release and no further modifications were observed (Schemes 2B.3 and 3C).

In summary, the commercially available clickable groups tetrazine and strained alkynes show unsatisfactory compatibility with the reactive groups of the HIPS and Knoevenagel building blocks (*N*,*N*′-dimethylhydrazine and pyrazolone). Hence, the azides **6**, **12**, and **13** remained as the most promising candidates.

FGE-mediated formylglycine formation in proteins

We used designed ankyrin repeat protein (DARPin) E01 (Figure S10), which is directed against the epidermal growth factor receptor (EFGR),[57] as a model protein for conjugation. The enzymatic conversion of the CTPSR target sequence in a C-terminally CTPSR-His_6-tagged DARPin was performed in a bicine buffer containing 200 mM arginine with 10 mol% of CTPSR-tagged FGE from *Mycobacterium tuberculosis* (MtFGE), $CuSO_4$ and $CaCl_2$ (each 10 μM) for 16–20 h at 22–25 °C (Figure 1A). Copper and calcium salts were added for *in situ* FGE reconstitution. The CTPSR-tag within FGE serves as an internal standard for FGly conversion and conjugation reactions. Protein mixtures were directly treated with trypsin and the fragments analyzed by MALDI-ToF-MS to determine the FGly modification of the DARPins (Figure 1B). Since FGly formation leads to a mass shift of −18 Da, intramolecular imine formation between FGly and the N terminus of peptides produces a detectable Schiff base in MALDI-ToF-MS. Integration of the peaks corresponding to the CTPSR-tag containing peptide (m/z_{obs} 2736.7, m/z_{calc} 2736.3), FGly-peptide (m/z_{obs} 2718.6, m/z_{calc} 2718.3), and the intramolecular imine (m/z_{obs} 2700.6, m/z_{calc} 2700.3) revealed a conversion of approximately > 95 % assuming similar ionization efficiencies for all three species.[28] The almost quantitative conversion could also be shown by subsequent conjugation with azide **12** and the absence of the starting material band in SDS-PAGE analysis (see below, Figure 2D). Subsequently, the FGly-containing DARPin was rebuffered either into HIPS ligation buffer (100 mM phosphate, 20 mM NaCl, pH 6.0) or Knoevenagel ligation buffer (50 mM citrate, 50 mM NaCl, pH 7.2). However, precipitation of DARPin was observed in the HIPS buffer, which is probably due to the pH (6.0) close to the isoelectric point of the protein (pI_{calc}: 4.96).

Direct fluorophore conjugation with HIPS-CF (2) and *trapped* Knoevenagel-CF (9) requires large excess of reagent

In order to compare the conjugation efficiencies of the standard HIPS and *trapped* Knoevenagel ligations with our modular approach involving bifunctional linkers, 30 μM of the FGly-containing DARPins were incubated with different equivalents of the 5(6)-carboxyfluorescein derivatives **2** and **9**. Samples were taken after 2, 6, 10, and 24 h, which were then analyzed by reducing SDS-PAGE (15 %) and in-gel fluorescence imaging (Figures 1C, S12 and S13). Multiple bands at approx. 16 kDa were observed for the unconjugated FGly-DARPin. These could result from conformational changes (internal imine formation) or fragmentation; the latter is known from published peptide experiments.[58] The addition of arginine during FGly-conversion and SDS-PAGE analysis probably stabilizes the FGly-containing DARPin through imine formation, and indeed less fragmentation was observed (Figure S11). Therefore, this additive was always included preventively during FGly conversion.

The success of the fluorescence labeling by standard HIPS and Knoevenagel ligation with the carboxyfluorescein derivatives **2** and **9** was proven by the selective formation of a protein

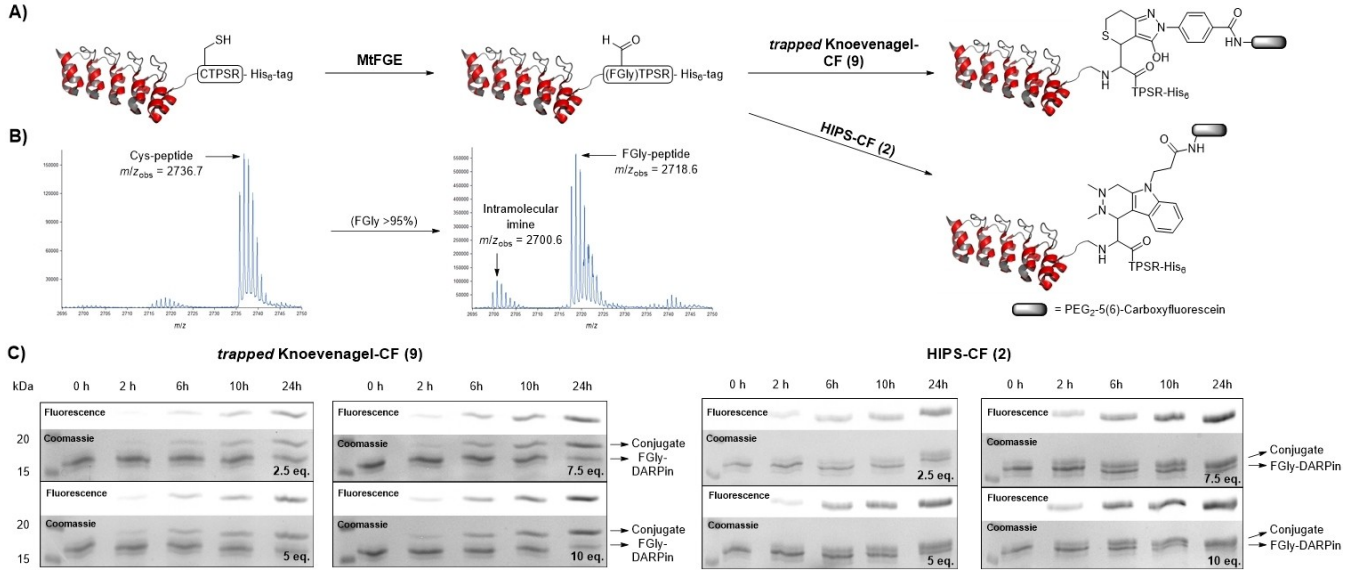

Figure 1. Stoichiometry- and time-dependent conjugation assay with HIPS-CF (**2**) and *trapped* Knoevenagel-CF (**9**). A) Bioconjugation experiments: DARPin-CTPSR-His_6 (100 μM) was enzymatically oxidized in a bicine buffer containing 10 mol% $CuSO_4$ and 10 mol% CTPSR-MtFGE. The FGly-containing DARPin was re-buffered (HIPS: 100 mM phosphate, 30 mM NaCl, pH 6.0; Knoevenagel: 50 mM citrate, 50 mM NaCl, pH 7.2) and subsequently fluorescence labeled using **2** and **9** (30 μM FGly-DARPin). B) MALDI-ToF analysis of relevant Cys- (*m/z* 2736.6) and FGly-containing peptides (*m/z* 2718.6 and 2700.6). C) SDS-PAGE analysis (15%) of stoichiometry- (2.5, 5, 7.5 and 10 equiv) and time-dependent conjugation assays. Samples (15 μg) were taken after 2, 6, 10 and 24 h and analyzed on gel by fluorescence (upper panels) before Coomassie staining (lower panels). Whole SDS gels and fluorescence images can be found in Figures S12 and S13.

band at higher molecular masses and increased fluorescence intensity over the time (Figure 1C, S12 and S13). In our experiments, 2.5–10 equivalents of **2** or **9** and 24 h were not sufficient to achieve full conversion at 30 μM, assuming a similar low reactivity for the HIPS and *trapped* Knoevenagel ligation reaction. Full conversion was obtained when 10 equivalents of **9** were used at higher protein concentrations (100 μM; Figure S14). Therefore, high concentrations and an excess of the payload-containing building blocks are needed for the standard HIPS and Knoevenagel ligation at low concentrations. Due to the complex and usually expensive multistep synthesis towards drugs, fluorophores or other payloads a more efficient procedure needs to be developed.

Conjugation with azide-containing bifunctional linkers gives superior results

In order to demonstrate an alternative route towards FGly-based bioconjugations with higher efficiencies, proof-of-concept experiments with the bifunctionalized HIPS- and *tandem* Knoevenagel-azides **6** and **12** were performed in the same buffers described above. In both cases, the reagent was added to the target proteins and incubated either for 16 h at 30 °C with 2 mM of **6** or 24 h at 22 °C with 10 mM of **12** (Scheme 4).

Conjugated DARPins were subsequently rebuffered into phosphate buffer (8% DMSO, 100 mM phosphate, 150 mM NaCl, pH 7.2) to remove excess reagent. DMSO was added for

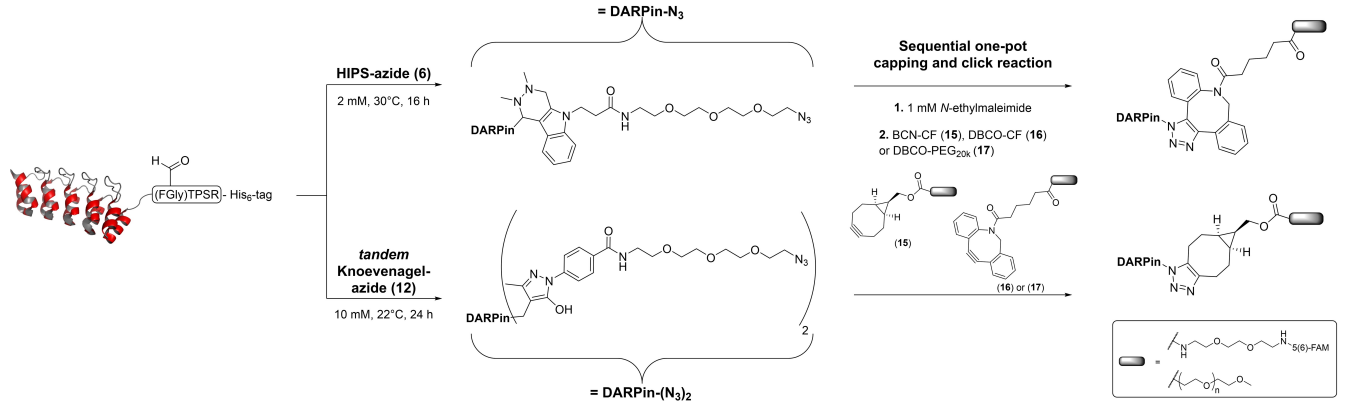

Scheme 4. Azide-derivatization of DARPin by HIPS-azide (**6**) and *tandem* Knoevenagel-azide (**12**). FGly-DARPin was first conjugated with HIPS-azide (**6**, 2 mM, 16 h, 30 °C) or *tandem* Knoevenagel-azide (**12**, 10 mM, 24 h, 22 °C), rebuffered in phosphate buffer (100 mM phosphate, 150 mM NaCl, pH 7.2, 8% DMSO), and then used in a sequential one-pot capping and click reaction with different strained alkynes.

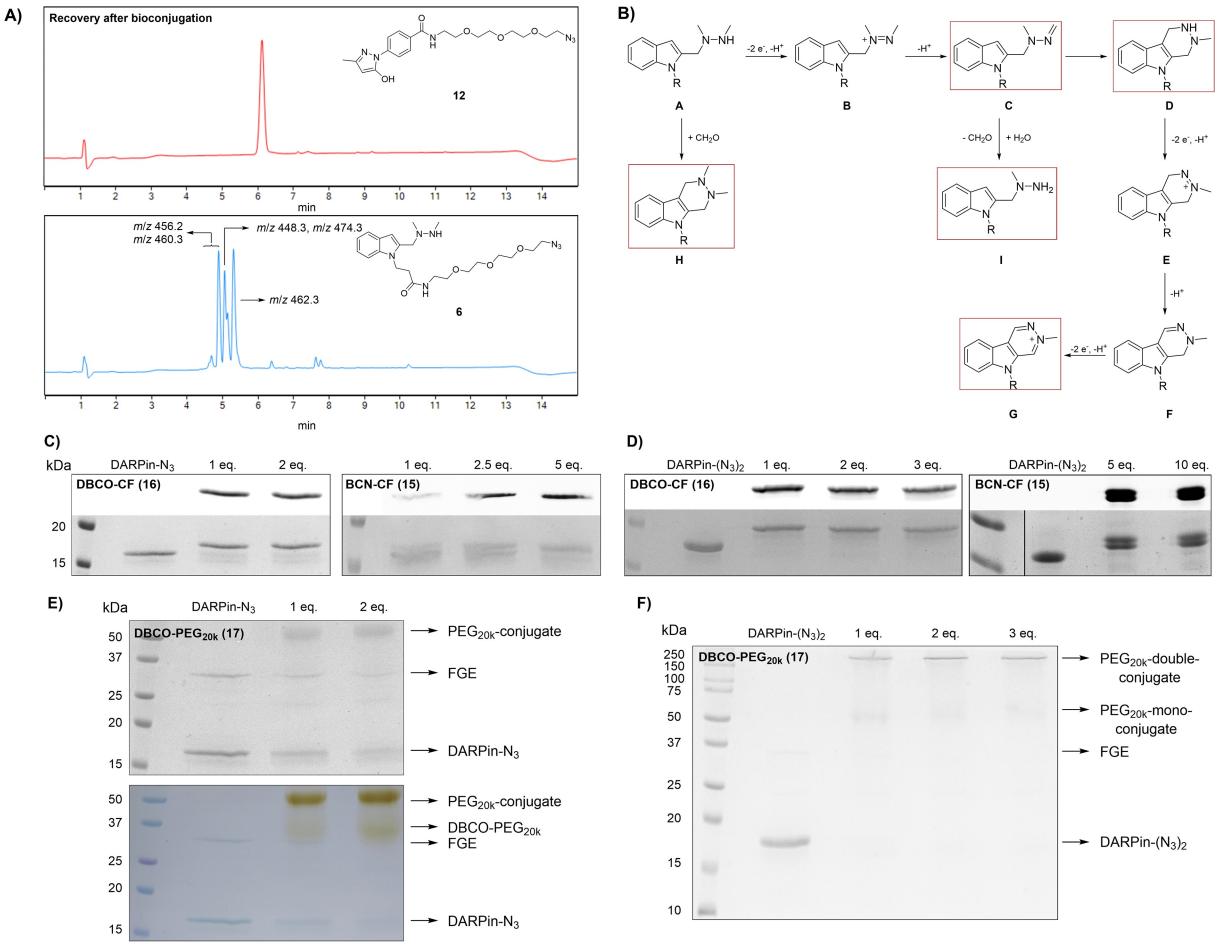

Figure 2. Recovery of the bifunctional reagents **6** and **12** after bioconjugation and subsequent SPAAC experiments. A) LC–MS analysis of recovered *tandem* Knoevenagel-azide (**12**) and HIPS-azide (**6**) after PD10 and extraction. B) Possible mechanism for oxidative decomposition and modifications of **6**. C), D) SDS-PAGE analysis (15%; lower panels) and in-gel fluorescence (upper panels) of DARPin-N_3, DARPin-$(N_3)_2$ and subsequent click reactions with different equivalents of BCN-CF (**15**) and DBCO-CF (**16**). On the right of D, MW markers and samples are from the same SDS gel. Only relevant samples are shown. Full SDS gels and fluorescence images of C and D can be found in Figure S15 and S16. E), F) SDS-PAGE analysis (15%) of DARPin-N_3, DARPin-$(N_3)_2$ and subsequent click reaction with different equivalents of DBCO-PEG_{20k} (**17**). PEGylation was further analyzed with a PEG-specific $BaCl_2/I_2$ staining protocol.

improved solubility of the DBCO- and BCN-modified payloads. Additionally, the fractions with excess azide were also collected, freeze dried, extracted with dichloromethane (CH_2Cl_2) and analyzed by LC–MS (Figure 2A). Interestingly, **12** could be recovered with 94% and good purities, while **6** underwent decomposition (Figure 2A and 2B). In our postulated decomposition mechanism, a two-electron oxidation and subsequent deprotonation leads to the formation of the hydrazone **C** (m/z_{calc} 460.27 ($[M+H]^+$)), which could induce an intramolecular attack of the indole to form hydrazine **D** (m/z_{calc} 460.27 $[M+H]^+$). Another two-electron oxidation, deprotonation and a third two-electron oxidation finally results in the formation of the diazacarbazol derivative **G** (m/z_{calc} 456.24 $[M]^+$). This aromatic structure cannot undergo further electron release.[59] Further signals might occur due to the hydrolytic release of formaldehyde by intermediate **C** to **I** (m/z_{calc} 448.27 $[M+H]^+$), which can then be incorporated by another molecule of **A** to form **H** (m/z_{calc} 474.28 $[M+H]^+$). These postulated species are in accordance with results published by T. Linz et al.[60] Moreover, partial in source-fragmentation and elimination of the hydrazine moiety was used to corroborate the postulated species (Figures S22–S26). Additionally, the compound corresponding to *m/z* 456.24 shows higher ionization efficiency and increased absorption at higher wavelength (254 and 280 nm) compared to the other signals, indicating formation of an expanded and positively charged aromatic structure (Figure S21).

To elucidate the source of the oxidant, HIPS-azide (**6**) was diluted in HIPS ligation buffer (100 mM phosphate, 30 mM NaCl, pH 6.0) and incubated for 16 h at 30 °C with different additives and analyzed by LC–MS. Without any additives partial decomposition was observed, while the compound was completely stable upon addition of EDTA to the buffer. The opposite was observed upon the addition of copper salts (e.g., $CuSO_4$), while exclusion of oxygen did not lead to slower oxidation.

Accelerated decomposition occurred in the presence of the FGly-containing DARPin, which is probably due to the coordination of $CuSO_4$ during the FGly conversion. Preventive treatment of the FGly-protein with EDTA could be considered to remove

coordinated copper and reduce HIPS decomposition (Figure S20).

In summary, these experiments show that the oxidative decomposition of the hydrazine is caused by metal ions, able to serve as electron acceptors.

Efficient mono-conjugation with HIPS-azide (6)

In order to identify the most suitable and commercially available strained alkyne for the conjugation with aliphatic azides, 10 μM of DARPin-N_3, generated using **6**, were treated with different equivalents of BCN-CF (**15**) or DBCO-CF (**16**; Figure 2C and S15). Prior to the addition of any conjugation reagent, residual free thiols were treated in a sequential one-pot capping and click reaction with 1 mM *N*-ethylmaleimide to avoid thiol-yne side reactions. SDS-PAGE analysis of conjugated DARPin (Figure 2C and S15) revealed that DARPin-N_3 contains a faint fragmentation band at lower molecular masses, indicating that the protein was not fully converted to the azide. Qualitative analysis of tryptic peptides using MALDI-ToF-MS shows only minor amounts of unconjugated FGly-DARPin (Figure S27). Nevertheless, treatment with one or two equivalents of **16** for 3 h at 22 °C resulted in a prominent fluorescent protein band at approximately 19 kDa, confirming successful application of the modular conjugation protocol. Despite longer reaction times (22 h), the click reaction with BCN-CF (**15**) resulted in comparably lower conjugation efficiencies. At least 5 equivalents were necessary for complete conversion at low concentrations (Figure 2C and S15).

Tandem Knoevenagel-azide (12) allows efficient double conjugation

Compared to DARPin-N_3, the diazido substituted DARPin (DARPin-$(N_3)_2$), generated using the *tandem* Knoevenagel building block **12**, did not show any protein bands possibly originating from fragmentations or residual starting material, indicating almost full conversion to the conjugate (Figure 2D and S16). Additionally, MALDI-ToF-MS analysis detected only traces of the FGly-DARPin (Figure S28). The following click reaction of DARPin-$(N_3)_2$ with the reactive dye DBCO-CF (**16**) was performed under similar conditions (22 °C for 3 h) and almost full conversion to the double-conjugate was observed upon addition of one equivalent per azide. A faint fluorescent protein band below the double-conjugate is assigned to the mono-conjugate (Figure 2D and S16). These results and efficiencies are in agreement to previous reports on diazido substituted linkers, which were attached to antibodies by transglutaminase.[61] Due to the lower reactivity of BCN,[62] the conjugation tests with DARPin-$(N_3)_2$ were carried out at higher concentrations (50 μM) and 5 or 10 equivalents per azide of BCN-CF (**15**) were applied. Despite the utilization of higher concentrations, longer reaction times (16 h) and modified stoichiometry, no complete conversion to the double-conjugate was observed. Here, approximately 50% mono- and 50% double-conjugate were obtained (Figure 2D and S16). Even an increase to 50 or 100 equivalents did not lead to complete double-conjugation (Figure S17–S19). A reason for incomplete conversion to the double-conjugate could be the relatively lower reactivity towards aliphatic azides and also the inherent instability of the alkyne moiety (see above).

Further click reactions with the less reactive and commercially available DBCO-PEG_{20k} (**17**) were performed to demonstrate the efficiency of the modular system (Figure 2E and F). In general, higher concentrations, temperatures, and longer reaction times are recommended for this reactive group.

For example, DARPin-N_3 (10 μM) was treated for 16 h at 37 °C with one or two equivalents of **17**. In addition to Coomassie staining, SDS-PAGE analysis was also performed using a PEG-specific $BaCl_2/I_2$ staining protocol (Figure 2E).[63,64] In both reactions, a major PEGylated protein band was observed with an apparent molecular mass of approximately 50 kDa ($MW_{calc} = 38.6$ kDa). The deviation of the predicted molecular mass of a conjugated DARPin can be explained by the larger hydrodynamic radius of the bound PEG.[65] Additionally, DARPin-$(N_3)_2$ was treated with 1–3 equivalents per azide of **16** (Figure 2F). With one equivalent, the double-PEGylated protein can be observed as a major protein band at 200 kDa. However, the mono-conjugate can still be detected at 50 kDa. By increasing the equivalents to 3 per azide, almost full conversion to the doubly PEGylated protein was obtained (Figure 2F). In conclusion, our modular approach allows the efficient synthesis of linear or branched PEG linkers.

Strained alkynes and tetrazines gave insufficient results

Further conjugation tests were also performed with HIPS-DBCO (**4**) and HIPS-BCN (**5**) by incubating the FGly-DARPin (56 μM) with 590 μM of **4** or **5**. Higher concentrations were not possible due to limited solubilities of both reagents. The mixture was incubated at 22 °C overnight and directly analyzed after tryptic digest by MALDI-ToF-MS (Figure 3A). It could be shown that both HIPS reagents were successfully conjugated to the protein, but starting material could still be detected, corresponding to incomplete ligation. Furthermore, in both reactions a signal with a relative mass shift of +18 Da was detected, indicating acid-mediated alkyne hydration forming a ketone (Scheme 2B.2). Larger amounts of the water adduct can be observed for BCN, which probably is more prone to protonation due to the comparatively electron-rich character of the strained alkyne.[62] Prolonged incubation times during the HIPS ligation (pH 5.5–6.5) could be a reason for this side product. Further incubation with an azide functionalized payload yielded only traces of the desired conjugate. As previously assumed, strained alkynes seem to be not compatible under these mild HIPS ligation conditions.

Compared to aliphatic azides, aryl azides and tetrazines show higher reactivities towards BCN.[49,62] Hence, the *tandem* Knoevenagel constructs **13** and **14** (final concentration of 2.5 mM) were used for DARPin conjugation. Due to their limited solubility, 10% of DMSO was added. After incubation for 24 h at

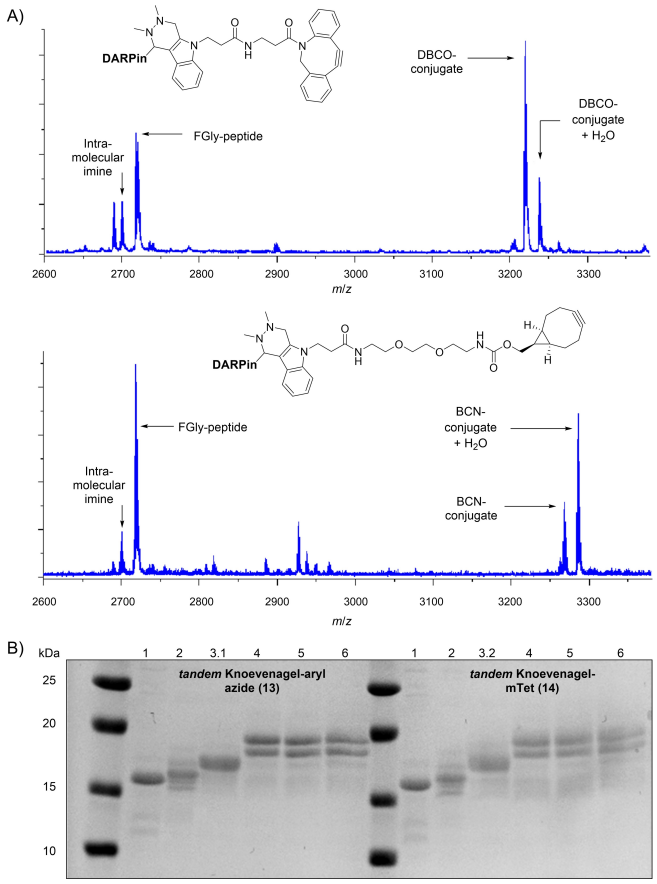

Figure 3. Analysis of the conjugation with HIPS reagents **4** and **5** and *tandem* Knoevenagel reagents **13** and **14**. A) MALDI-ToF-MS analysis of DARPin conjugated to **4** and **5** showing tryptic peptides, indicating incomplete ligation and water addition to the strained alkyne. B) Coomassie-stained SDS-PAGE (15%) analysis of DARPin conjugated to **13** and **14** and subsequent click reaction with BCN-CF (**15**). 1) DARPin-CTPSR-His_6, 2) FGly-DARPin, 3.1) DARPin-$(aryl\ azide)_2$, 3.2) DARPin-$(mTet)_2$, 4) 2.5 equiv. of **15** per azide, 5) 5 equiv/azide, 6) 10 equiv/azide.

22 °C and rebuffering into the above described phosphate buffer, 50 μM of the conjugated DARPins were treated with 2.5, 5, and 10 equivalents per azide of BCN-CF (**15**). Both DARPin-$(aryl\ azide)_2$ and DARPin-$(mTet)_2$ did not show any protein bands corresponding to starting material, indicating full conversion (Figure 3B). Despite the large excess of **15** used in the subsequent click reactions, incomplete conversion to the double-conjugate was revealed by SDS-PAGE analysis (Figure 3B). Here, approx. 50% mono- and 50% double-conjugate were obtained, indicating that BCN cannot be used for the conjugation of two azides or tetrazine, which are in close proximity.

We were able to establish a highly efficient modular conjugation system for mono- and double-conjugation, which requires a simple and inexpensive azide modified HIPS or *tandem* Knoevenagel building block and stoichiometric amounts of DBCO-derivatives, while BCN-derivatives are less effective. Another advantage of this modular system is that these azides and the azide-labeled proteins can be stored in solution for several months at −80 °C.

Live-cell fluorescence imaging

Finally, to test an appropriate application for the modular conjugation strategy and to analyze the impact of this artificial modification, live-cell imaging experiments with fluorescently labeled DARPins were conducted (Figure 4). A431 and MCF7 cells, which present either high or low levels of EGFR, respectively, were incubated with DARPin-CF (generated using **9**) or DARPin-$(CF)_2$ (generated using **12** and **16**) and analyzed by confocal fluorescence microscopy.[66] Both conjugates bound to A431 cells (Figure 4A and D), but not to MCF7 cells (Figure 4C and F), which indicates that specific EGFR targeting of the aldehyde-tagged DARPin is maintained after the modification by *trapped* or *tandem* Knoevenagel reactions.[57] Internalization and colocalization with lysosomes have been observed for both DARPin conjugates at 37 °C (Figure 4A and D) but not at 4 °C (Figure 4B and E) suggesting that selective EGFR-mediated endocytosis occurs.[67] Analysis of the mean fluorescence intensity of live-cell images taken at the same temperature revealed about a twofold increased value for DARPin-$(CF)_2$ compared to DARPin-CF (Figure 4). Hence, conjugating the DARPin with two carboxyfluorescein units via the *tandem* Knoevenagel reaction significantly improves the signal-to-noise

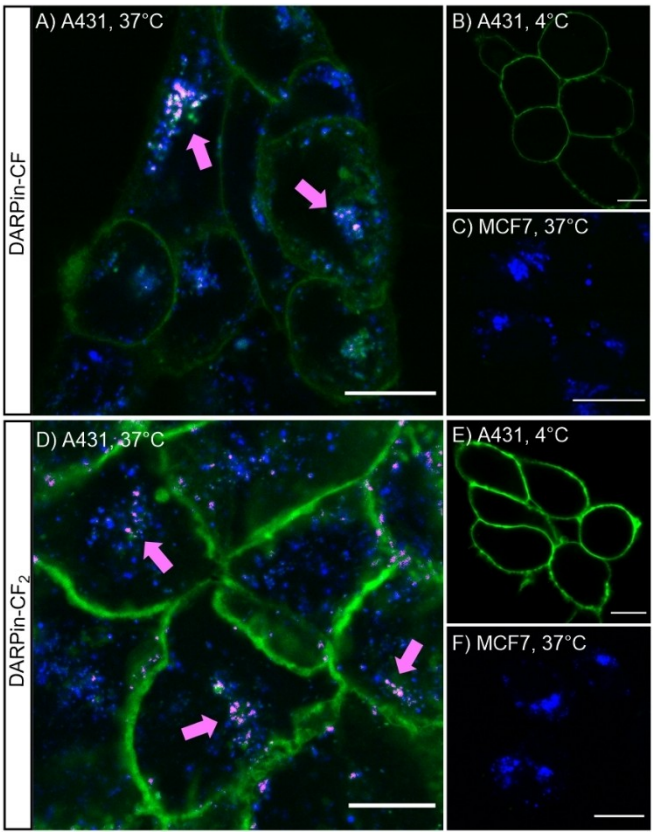

Figure 4. Live-cell imaging of DARPin conjugates. A), D) A431 cells at 37 °C, B), C) A431 cells at 4 °C, and E), F) MCF7 cells at 37 °C were incubated with 100 nM DARPin-CF (A–C) or DARPin-CF_2 (D–E) for 6–8 h. Fluorescence of 5(6)-carboxyfluorescein and LysoTracker DND-22 are shown in green and blue, respectively. For images with merged channels, colocalization is pseudo-colored in magenta and indicated by arrows. Scale bars: 15 μm.

ratio for fluorescence-based studies (Figure S29). In contrast to the standard Knoevenagel ligation (100 μM, 10 equiv), this modular approach allows protein labeling with stoichiometric amounts of the fluorophore. Live-cell imaging experiments demonstrated that both DARPin conjugates retain the ability of EGFR binding and successive EGFR-mediated internalization.

Conclusion

Fluorescence labeling of C-terminal-His_6-tagged DARPin E01 by the aldehyde-tag strategy combined with standard HIPS or *trapped* Knoevenagel reactions is compromised by slow kinetics and the need of a large excess of the expensive conjugation building block at low concentrations. In our experiments, 2.5 to 10 equivalents of HIPS-CF (**2**) and *trapped* Knoevenagel-CF (**9**) and 24 h were not sufficient for complete conjugation of protein as detected by SDS-PAGE. However, similar efficiencies for HIPS- and Knoevenagel ligations were obtained.

Therefore, we established a straightforward synthesis of different bifunctional HIPS and *tandem* Knoevenagel building blocks capable of being used in bioorthogonal click reactions. In contrast to the azide derivatives, tetrazine-, BCN- and DBCO-derivatization led to several side reactions involving the hydrazine or pyrazolone. However, azide derivatives showed sufficient chemical orthogonality. They can be stored at −80 °C in solution for several months, and efficiently conjugated to target proteins.

Azide-modified DARPins were treated with DBCO-PEG_{20k} (**17**) and DBCO-5(6)-carboxyfluorescein (**16**) and full conversion was attained with almost equimolar amounts of the DBCO-containing building blocks. Additionally, a branched PEG linker using linear DBCO-PEG was obtained (Table 1).

Finally, the impact of one- and twofold fluorescence labeling on binding behavior was tested by live-cell fluorescence imaging. Treatment of A431 cells (high EGFR expression) and MCF7 cells (low EGFR expression) with DARPin-CF and DARPin-CF_2 resulted in selective receptor-mediated endocytosis. Furthermore, a better signal-to-noise ratio was obtained with DARPins modified with two molecules of carboxyfluorescein.

All in all, the presented combination of HIPS and Knoevenagel ligation with click chemistry shows high efficiencies and opens up new synthetic strategies to complex protein conjugates. This method could be well suited to generate PEGylated therapeutic proteins with improved pharmacokinetics or to produce homogenous antibody–drug conjugates with a drug-to-antibody ratio of 2 or 4 for one aldehyde tag at, for example, the heavy chain.

The modular system can be used for the labeling of living cells or proteins in the lysate. For such experiments, FGly can be introduced by co-expression with FGE. However, a limiting factor in the lysate are small molecules containing aldehyde moieties. Such in vivo experiments are part of our current research.

Table 1. Compatibility aspects of the bifunctional building blocks utilized in this study. Classification is based on the assessment of the obtained results.

	Additional reactive group	Synthetic accessibility	Solubility	Stability	Conjugation efficiency
HIPS	aliphatic azide (**6**)	+	+	o	+/o
	DBCO (**4**)	o	o	o	–
	BCN (**5**)	o	o	–	–
	mTet (**3**)	–		–	
tandem Knoevenagel	aliphatic azide (**12**)	+	+	+	+
	aromatic azide (**13**)	+	o	+	o/–
	mTet (**14**)	o	o	o	o/–

Experimental Section

General information: Reactions sensitive to oxygen and moisture were performed using Schlenk technique and under argon. Chemicals and solvents were bought from commercial sources and used without further purification. Anhydrous solvents were obtained through distillation over desiccant. For extraction and column chromatography, distilled EtOAc and petroleum ether were used. Column chromatography was performed with silica gel with a diameter of 0.040–0.063 mm (Merck). For substance detection, aluminum-plates with silica gel 60 and fluorescence-indicator F254 by Merck and UV radiation (254 nM) and/or staining solutions (bromocresol, potassium permanganate or ninhydrin) were used. HPLC analysis were conducted on an Agilent 1200 series LC–MS system with a C_{18} column Luna (100×2 mm, particle size 3 μm, Phenomenex) using a linear acetonitrile gradient from 5–95% in 12 min (+0.1% formic acid). HPLCs were monitored at 220 nm. For preparative RP-HPLC, a LaChrom HPLC system (Merck Hitachi) with Interface D-7000, UV detector L-7520 and pump L-7150 was used. Purifications were performed with a C_{18} Jupiter column (250× 21.2 mm, particle size 10 μm, flowrate 10 mL/min, Phenomenex). ^1H and ^{13}C NMR spectra were obtained with a Bruker DRX 500 or BRUKER Avance 500. The measurements were carried out at 298 K and processed using $Mest_R$eNova (MestreLab). Chemical shifts are given relative to residual solvent signals. The multiplicities are given as s (singlet), d (doublet), t (triplet), q (quartet) and m (multiplet) with coupling constants given in Hertz.

Chemical synthesis: The chemical synthesis of the Knoevenagel core segment **8**, HIPS-CF (**2**), HIPS-DBCO (**4**), clickable precursors, fluorescein modifications and PEG linkers were performed similar to procedures describe in the literature and can be found in the supporting information. The synthesis of the HIPS core segment **1** is already described in our previous publication.[28]

Fmoc-HIPS-mTet: Fmoc-HIPS (**1**, 45 mg, 0.09 mmol) was dissolved in CH_2Cl_2/DMF (9:1, *v/v*, 4 mL) and HOBt (16 mg, 0.12 mmol) was added. Then, the obtained solution was combined with (4-(6-methyl-1,2,4,5-tetrazin-3-yl)phenyl)methanamine hydrochloride

(45 mg, 0.19 mmol) and triethylamine (50 μL, 0.36 mmol) and the start of the reaction was induced by the addition of EDC·HCl (56 mg, 0.29 mmol). The mixture was stirred overnight at RT until a mixture of petroleum ether/ethyl acetate (1:1, *v/v*, 30 mL) was added. The red suspension was washed three times with $KHSO_4$ solution (0.5 M, 30 mL each) and three times with saturated $NaHCO_3$ solution (30 mL each). The organic layer was dried over $MgSO_4$ and the solvent was removed *in vacuo*. The desired product was isolated as a red solid (25 mg, 0.04 mmol, 44%). LC–MS (ESI+): *m/z* calcd for $C_{39}H_{39}N_8O_3$ $[M+H]^+$: 667.31, found: 667.31 (t_R = 11.5 min).

Fmoc-HIPS-BCN: **1** (65 mg, 0.13 mmol) and pentafluorophenol (33 mg, 0.18 mmol) were dissolved in ethyl acetate (abs., 3 mL) and cooled down to 0 °C. Next, DIPEA (30 μL, 0.18 mmol) and solid DCC (29 mg, 0.14 mmol) were added and the reaction mixture was stirred for 2.5 h at RT. After stirring, the obtained suspension was again cooled to 0 °C, the precipitate was filtered off and the filter cake was washed with cold ethyl acetate (10 mL). Subsequently, the filtrate was washed two times with dH_2O (10 mL each) and two times with saturated sodium chloride solution (10 mL each). The organic layer was dried over Na_2SO_4 and concentrated *in vacuo*. The crude HIPS-PFP ester (116 mg) was then used without further purification.

In parallel, BCN-NH_2 (25 mg, 0.08 mmol) and HIPS-PFP were dissolved in DMF (0.8 mL each), combined under argon and stirred for 20 h at RT. Afterwards, the solvent was removed *in vacuo* leading to the formation of a brownish, solid residue. The residue was dissolved in a mixture of water and acetonitrile (1:1, *v/v*, 2 mL) and directly purified by RP-HPLC with a linear acetonitrile gradient (5–95% in 50 min, 0.1% TFA). Lyophilization of product-containing fractions enabled the isolation of Fmoc-HIPS-BCN as a colorless solid (40 mg, 0.05 mmol, 63%). LC–MS (ESI+): *m/z* calcd for $C_{46}H_{56}N_5O_7$ $[M+H]^+$: 790.42, found: 790.46.

HIPS-BCN (5): Fmoc-HIPS-BCN (11.0 mg, 13.9 μmol) was dissolved in a solution of dioxane/methanol/2 M NaOH (10:9:1, *v/v/v*, 1.5 mL) and stirred for 30 min at RT. The solution was directly purified by RP-HPLC using a linear acetonitrile gradient (5-95% in 50 min). Lyophilization of product-containing fractions enabled the isolation of **5** as a pale-yellow solid (4.6 mg, 8.1 μmol, 58%). LC–MS (ESI+): *m/z* calcd for $C_{31}H_{46}N_5O_5$ $[M+H]^+$: 568.34, found: 568.35 (t_R = 7.2 min). HRMS (ESI+): *m/z* calcd for $C_{31}H_{46}N_5O_5$ $[M+H]^+$: 568.3494, found: 568.3497.

Fmoc-HIPS-azide: **1** (50 mg, 103 μM), HOAt (17.6 mg, 129 μmol), 1-amino-11-azido-3,6,9-trioxaundecane (45.1 mg, 207 μmol) and DIPEA (72 μL, 413 μmol) were dissolved in CH_2Cl_2/DMF (9:1, 1 mL) and afterwards EDC·HCl (59.5 mg, 310 μmol) was added portionwise. The mixture was stirred for 5 h at RT, concentrated *in vacuo* and finally diluted with DMF. After RP-HPLC and lyophilization, Fmoc-HIPS-azide (52 mg, 74%) was isolated as a brown oil. LC–MS (ESI+): *m/z* calcd for $C_{37}H_{46}N_7O_6$ $[M+H]^+$: 684.35, found: 684.35 (t_R = 11 min). HRMS (ESI+): *m/z* calcd for $C_{37}H_{45}N_7O_6Na$ $[M+Na]^+$: 706.33235, found: 706.3321.

HIPS-azide (6): Fmoc-HIPS-azide (50 mg) was dissolved in a solution of 20% piperidine in THF (2.3 mL) and stirred for 1 h at RT. Water was added to the reaction mixture until a colorless precipitate formed. The solid was filtered off and the filtrate was concentrated *in vacuo* and the residue was freeze-dried. Finally, the lyophilizate (25.9 mg, 77%) could be directly employed for bioconjugations, since LC–MS analysis revealed >95% purity and significant degradation during purification by RP-HPLC were observed. Moreover, due to rapid oxidative decomposition of purified **6**, the obtained oil was immediately dissolved in a mixture of water and acetonitrile (1:1, *v/v*) to a final concentration of 1 M and aliquots of that solution were stored at −80 °C until further use in bioconjugation reactions. LC–MS (ESI+): *m/z* calcd for $C_{22}H_{36}N_7O_4$ $[M+H]^+$: 462.28, found: 462.32 (t_R = 5.2 min). HRMS (ESI+): *m/z* calcd for $C_{22}H_{36}N_7O_4$ $[M+H]^+$: 462.28233, found: 462.2839.

Trt-*trapped* Knoevenagel-CF: A solution of Trt-*trapped* Knoevenagel-acid (**8**, 100 mg, 197.7 μmol), HATU (75 mg, 197.2 μmol) and DIPEA (33.5 μL, 197.5 μmol) in DMF (0.5 mL) was stirred for 5 min before a solution of H_2N-PEG_2-5(6)-CF (118 mg, 217.7 μmol) and DIPEA (70.5 μL, 414.75 μmol) in DMF (0.5 mL) was slowly added. After stirring for 4 h, the reaction mixture was directly purified by preparative RP-HPLC. The product (110 mg, 55%) was obtained as a yellow solid. LC–MS: *m/z* calcd for $C_{58}H_{51}N_4O_{10}S$ $[M+H]^+$: 995.33, found: 995.32 (t_R = 10.1 min). HRMS: *m/z* calcd for $C_{58}H_{51}N_4O_{10}S$ $[M+H]^+$: 995.33204, found: 995.3301.

***Trapped* Knoevenagel-CF (9)**: Trt-*trapped* Knoevenagel-CF (20 mg, 20.1 μmol) was suspended in CH_2Cl_2 (670 μL) with DMF (3 drops), H_2O (50 μL) and TIPS (51.4 μL). The reaction mixture was cooled to 0 °C und TFA (410 μL) was slowly added. After 2.75 h of stirring at 0 °C, DMF (3 mL) was added, CH_2Cl_2 removed under vacuum and then directly purified by RP-HPLC. The product (12.6 mg, 83%) was obtained as a yellow solid. LC–MS: *m/z* calcd for $C_{39}H_{36}N_4O_{10}S$ $[M+H]^+$: 753.22, found: 753.26 (t_R = 7.9 min). HRMS: *m/z* calcd for $C_{39}H_{36}N_4O_{10}S$ $[M+H]^+$: 753.22249, found: 753.2219.

***Tandem* Knoevenagel-methyl ester**: Ethyl 3-oxobutanoate (587 mg, 4.51 mmol), methyl 4-hydrazinobenzoate (750 mg, 4.51 mmol), and sodium acetate (740 mg, 9 mmol) were suspended in AcOH (9 mL) and stirred for 3 h at 75 °C. After cooling to RT, the solvent was removed under reduced pressure and a brown solid was obtained. The crude was suspended in H_2O (25 mL) and extracted with CH_2Cl_2 (2×75 mL). The combined organic phases were washed with sat. $NaHCO_3$ (25 mL), brine (25 mL) and dried over $MgSO_4$. The solvent was removed under reduced pressure and the product (594 mg, 2.6 mmol, 57%) was obtained after column chromatography (eluent: EtOAc/PE 1:4) as a yellow solid. R_f = 0.2 (EtOAc/PE 1:3). ^{1}H NMR (500 MHz, $CDCl_3$, 25 °C) = 8.05 (d, ^3J = 8.5 Hz, 2H, Ar-**H**), 7.99 (d, ^3J = 8.6 Hz, 2H,Ar-**H**), 3.90 (s, 3H, -OC**H$_3$**), 3.45 (s, 2H, –C**H$_2$**–), 2.20 (s, 3H, –C**H$_3$**). ^{13}C NMR (126 MHz, $CDCl_3$) = 170.89 (N–**C**=O), 166.74 (–**C**O–OCH_3), 157.02 (N–**C**–CH_3), 141.90 (N–**C$_{Ar}$**), 130.69 (**C$_{Ar}$**–C_{Ar}–C=O), 126.17 (**C$_{Ar}$**–C=O), 117.74 (N–C_{Ar}–**C$_{Ar}$**), 52.16 (–CO–O**C**H_3), 43.27 (CH_3–CN–**C**H_2), 17.19 (–**C**H_3). LC–MS (ESI+): *m/z* calcd for $C_{12}H_{13}N_2O_3$ $[M+H]^+$: 233.09, found 233.12 (t_R = 7.5 min). HRMS (ESI+): *m/z* calcd for $C_{12}H_{12}N_2O_3Na$ $[M+Na]^+$: 255.07401, found 255.0739.

***Tandem* Knoevenagel-acid (11)**: *Tandem* Knoevenagel-methyl ester (500 mg, 2 mmol) was dissolved in 1 M NaOH (15 mL) and stirred for 3.5 h at RT. Afterwards, the reactions mixture was diluted with aq. HCl until pH of 4 was reached. The product (414 mg, 93%) was obtained through filtration as a beige-colored solid. R_f = 0.6 (CH_2Cl_2/MeOH/AcOH, 9:1:0.01). ^{1}H NMR (500 MHz, [D_6]DMSO, 25 °C, Iminol): 7.98 (d, ^3J = 8.7 Hz, 2H, Ar-**H**), 7.88 (d, ^3J = 8.6 Hz, 2H, Ar-**H**), 5.39 (s, 1H, CN–C**H**–C–OH), 2.13 (s, 3H, –C**H$_3$**). ^{13}C NMR (126 MHz, [D_6] DMSO): 171.71(–N–**C**=O), 166.87 (–**C**OOH), 166.82 (–**C**OOH) 159.37 (–**C**–CH_3), 153.92 (–N–**C**–OH), 149.08 (–**C**–CH_3), 142.49 (–**C$_{Ar}$**), 141.63 (–**C$_{Ar}$**), 130.48 (–**C$_{Ar}$**), 130.36 (–**C$_{Ar}$**), 126.49 (–**C$_{Ar}$**), 126.04 (–**C$_{Ar}$**), 119.23 (–**C$_{Ar}$**), 116.92 (–**C$_{Ar}$**), 88.20 (–CH_3–C–**C**H=), 43.16 (–CH_3–CN–**C**H_2–), 16.71 (–**C**H_3), 14.26 (–**C**H_3). LC–MS (ESI+): *m/z* calcd for $C_{11}H_{11}N_2O_3$ $[M+H]^+$: 219.07, found 219.09 (t_R = 5.6 min). HRMS (ESI+): *m/z* calcd for $C_{11}H_{12}N_2O_3Na$ $[M+Na]^+$: 241.05836, found 241.0578.

***Tandem* Knoevenagel-azide (12)**: H_2N-PEG_3-N_3 (75 mg, 34.4 μmol), HOAt (46.8 mg, 34.4 μmol), *tandem* Knoevenagel-acid (**11**, 50 mg, 22.9 μmol) and DIPEA (60 μL, 34.4 μmol) were dissolved in DMF (1 mL) under argon, and EDC·HCl (65.9 mg, 34.4 μmol) was added in

portions over 10 min. The reaction mixture was stirred overnight at RT and then directly purified by preparative RP-HPLC. After freeze drying, azide **12** (106 mg, 74%) was obtained as a yellowish solid. ^{1}H NMR (500 MHz, $CDCl_3$, 25 °C): 7.96 (d, ^3J = 8.4 Hz, 2H, Ar-**H**), 7.82 (d, ^3J = 8.5 Hz, 2H, Ar-**H**), 6.80 (s, 1H, -**NH-**), 3.63 (m, 14H, PEG), 3.44 (s, 2H, -CN-C**H$_2$**-C=O), 3.33 (t, ^3J = 5.1 Hz, 2H, N_3–C**H$_2$**–), 2.19 (s, 3H, C**H$_3$**). ^{13}C NMR (126 MHz, $CDCl_3$, 25 °C): 170.82 (–N–**C**=O), 166.90 (–C_{Ar}–**C**=O), 156.91 (CH_3–**C**–N), 140.68 (–**C$_{Ar}$**–N), 130.58 (–**C$_{ar}$**–C=O), 128.00 (–**C$_{Ar}$**–C_{Ar}-C=O), 117.97 (–**C$_{Ar}$**–C_{Ar}–N), 70.77 (PEG), 70.74 (PEG), 70.67 (PEG), 70.35 (PEG), 70.12 (PEG), 69.91 (PEG), 50.73 (–**C**H$_2$-N_3), 43.25 (–**C**H$_2$–C=O), 39.86 (PEG), 17.16 (–**C**H$_3$). LC–MS (ESI+): *m/z* calcd for $C_{19}H_{27}N_6O_5$ $[M+H]^+$: 419.20, found 419.22 (t_R = 6.3 min). HRMS (ESI+): *m/z* calcd for $C_{19}H_{26}N_6O_5Na$ $[M+Na]^+$: 441.18569, found 441.1849.

***Tandem* Knoevenagel PEG-amine trifluoroacetate**: *Tandem* Knoevenagel-azide (**12**, 50 mg, 119.5 μmol) was dissolved in THF (970 μL) and then PPh_3 (94 mg, 358.4 μmol) was added in portions. After stirring for 1 h at RT, H_2O (100 μL) was added and an orange suspension was obtained. To obtain better solubility, further THF (4 mL) and H_2O (400 μL) was added. After 17 h, only the iminophosphorane was detected by LC–MS, which is why the solution was acidified wit 1 M HCl until pH 1 was reached and then the solvent was removed under reduced pressure. Again, the iminophosphorane was obtained as the major product. Therefore, the crude was again dissolved in THF/H_2O (1:1, 5 mL) and heated to 60 °C for 3.5 h. Still iminophosphorane was detected, consequently AcOH was added until pH 4 was reached and then the reaction mixture was heated to 80 °C and stirred for 20 h. After removal of the solvent and preparative RP-HPLC, the product (45.5 mg, 75%) was obtained as a colorless oil. Amide/iminol ratio: 8:2. ^{1}H NMR (500 MHz, [D$_3$]ACN, 25 °C): 7.95 (d, ^3J = 8.8 Hz, 2H, Ar-**H**, amide), 7.88 (d, ^3J = 8.9 Hz, 2H, Ar-**H**, iminol), 7.86 (d, ^3J = 8.9 Hz, 2H, Ar–**H**, amide), 7.77 (d, ^3J = 8.7 Hz, 2H, Ar–**H**, iminol), 7.6 (s, 1H, N-**H**, iminol), 7.54 (s, 1H, N–**H**, amide), 7.34 (s, 3H, N**H$_2$**), 5.53 (s, 1H, –CN–**CH**=C–OH, iminol), 3.70 (m, PEG), 3.66 (m, PEG), 3.59 (m, PEG), 3.48 (s, 2H, –CN–C**H$_2$**–CO, amide), 3.13 (m, PEG), 3.09 (m, PEG), 2.24 (s, 3H, –C**H3**, iminol), 2.13 (s, 3H, -C**H$_3$**, amide). ^{13}C NMR: 172.65 (–N–**C**=O), 168.36 (–C_{Ar}–**C**=O), 168.04 (–C_{Ar}–**C**=O), 160.67 (–**C**–OH), 160.82 (TFA), 159.59 (–**C**–CH_3), 151.65 (–**C**–CH_3), 142.18 (–**C$_{Ar}$**–N), 139.95 (–**C$_{Ar}$**–N), 132.62 (–**C$_{Ar}$**–CO–NH–), 130.58 (–**C$_{Ar}$**–CO–NH–), 129.15 (–**C$_{Ar}$**–C_{Ar}–CO–), 129.07 (–**C$_{Ar}$**–C_{Ar}–CO–), 121.49 (–N–C_{Ar}–**C$_{Ar}$**), 118.36 (–N–C_{Ar}–**C$_{Ar}$**), 117.36 (TFA), 92.70 (–**C**H–C–OH), 70.90 (PEG), 70.86 (PEG), 70.80 (PEG), 70.73 (PEG), 70.70 (PEG), 70.64 (PEG), 70.51 (PEG), 70.45 (PEG), 67.27 (PEG), 43.90 (–**C**H$_2$–C–OH), 40.59 (PEG), 40.57 (PEG) 40.51 (PEG), 17.09 (–**C**H$_3$), 13.03 (–**C**H$_3$). LC–MS (ESI+): *m/z* calcd for $C_{19}H_{29}N_4O_5$ $[M+H]^+$: 393.21, found 393.25 (t_R = 3.9 min). HRMS (ESI+): *m/z* calcd for $C_{19}H_{29}N_4O_5$ $[M+H]^+$: 393.21325, found 393.2127.

***Tandem* Knoevenagel-aryl azide (13)**: *Tandem* Knoevenagel-PEG-amine trifluoroacetate (23.6 mg, 78.9 μmol), HOAt (16.1 mg, 118.5 μmol), 4-Azido-3,5-difluorobenzoic acid (23.6 mg, 118.5 μmol) and DIPEA (14 μL, 78.9 μmol) were dissolved in DMF (1 mL) under argon, and then EDC·HCl (65.9 mg, 34.4 μmol) was added in portions over 5 min. The reaction mixture was stirred overnight at RT in the dark. The product (30 mg, 66%) was directly purified by preparative RP-HPLC and obtained as a pale orange-colored solid. Amide/iminol ratio: 8:2. ^{1}H NMR (600 MHz, $CDCl_3$, 25 °C): 7.95 (d, ^3J = 8.8 Hz, 2H, Ar–**H**, amide), 7.80 (d, ^3J = 8.8 Hz, 2H, Ar-**H**, amide), 7.69 (m, 2H, Ar–**H**, iminol), 7.50 (m, 2H, Ar–**H**, iminol), 7.42 (m, 2H, N_3–Ar–**H**, amide), 7.36 (d, 2H, ^3J = 8.6 Hz, N_3–Ar–**H**, iminol), 7.20 (s, 1H, N–**H**), 7.00 (s, 1H, N–**H**), 5.64 (s, 2H, –CN–**CH**=C–OH, iminol), 3.63 (m, 16H, PEG), 3.46 (s, 2H,Pz-**H**, amide), 2.32 (s, 3H, C**H$_3$**, iminol), 2.21 (s, 3H, C**H$_3$**, amide). ^{13}C NMR (151 MHz, $CDCl_3$, 25 °C): 171.07 (–N–**C**O–CH_2–), 167.71 (–**C**O–NH–PEG), 164.75 (–NH–**C**O–C_{Ar}–C_{Ar}H–C_{Ar}F–), 160.64 (–N–**C**–OH), 157.27 (–N=**C**–CH_3), 156.10 (–**C$_{Ar}$**), 154.43 (–**C$_{Ar}$**), 150.01 (–N–**C**–CH_3), 140.85 (–CO–N–**C$_{Ar}$**), 136.75 (HO–C–N–**C$_{Ar}$**), 133.09 (–**C$_{Ar}$**–CO–NH-PEG), 131.13 (–**C**-F), 130.07 (–**C$_{Ar}$**–CO–NH-PEG), 128.46 (–**C$_{Ar}$**–C_{Ar}–CO–NH-PEG), 128.08 (–**C$_{Ar}$**–C_{Ar}–CO–NH-PEG), 121.67 (–N–C_{Ar}–**C$_{Ar}$**) 118.07 (–N–C_{Ar}–**C$_{Ar}$**), 111.43 (–NH–CO–C_{Ar}–**C$_{Ar}$**–C_{Ar}–F), 93.27 (–**C**H–C–OH), 70.52 (PEG), 70.48 (PEG), 70.29 (PEG), 70.24 (PEG), 69.83 (PEG), 69.68 (PEG), 43.31 (–**C**H$_2$–CO–), 40.19 (PEG), 40.04 (PEG), 17.16 (–**C**H$_3$), 12.33 (–**C**H$_3$). LC–MS (ESI+): *m/z* calcd for $C_{26}H_{30}F_2N_7O_6$ $[M+H]^+$: 574.22, found 574.24 (t_R = 8.1 min). HRMS (ESI+): *m/z* calcd for $C_{26}H_{29}F_2N_7O_6Na$ $[M+Na]^+$: 596.20396, found 596.2042.

***Tandem* Knoevenagel-PEG-*tert* butyl ester**: *Tandem* Knoevenagel-acid (**11**, 100 mg, 0.46 mmol), HOAt (93.6 mg, 0.69 mmol) and H_2N-PEG_3-COOtBu (181 mg, 0.68 mmol) were dissolved in DMF (1 mL) under argon, and then DIPEA (117 μL, 0.69 mmol) was added. Finally, EDC·HCl (131.8 mg, 0.69 mmol) was added in portions over 5 min. The reaction mixture was stirred overnight at RT before the product (90 mg, 42%) was purified directly by preparative RP-HPLC. Amide/iminol ratio: 20:1. ^{1}H NMR (600 MHz, $CDCl_3$, 25 °C): 7.96 (d, ^3J = 8.8 Hz, 2H, Ar-**H**), 7.84 (d, ^3J = 8.8 Hz, 2H, Ar-**H**), 7.04 (br s, 1H, N**H**) 3.96 (s, 2H, C**H$_2$**–COOtBu), 3.66 (m, 12H, PEG), 3.44 (s, 2H, –CN–C**H$_2$**–CO), 2.20 (s, 3H, C**H$_3$**), 1.44 (s, 9H, C(C**H$_3$**)$_3$). ^{13}C NMR (151 MHz, $CDCl_3$, 25 °C): 170.85 (–N–N–**C**O), 169.77 (–**C**OOtBu), 167.33 (–**C**O–NH), 156.92 (–N–**C**–CH_3), 140.75 (–N–N–**C$_{Ar}$**), 130.38 (–**C$_{Ar}$**–CO–NH), 128.12 (–**C$_{Ar}$**–C_{Ar}–CO–NH), 118.00 (–**C$_{Ar}$**–C_{Ar}–N–CO), 81.86 (–**C**(C**H$_3$**)$_3$), 70.73 (PEG), 70.64 (PEG), 70.62 (PEG), 70.32 (PEG), 69.94 (PEG), 69.06 (–**C**H$_2$-COOtBu), 43.28 (–**C**H$_2$–CO–N–), 40.03 (PEG), 28.21 (-C(**C**H$_3$)$_3$), 17.16 (–N–C–**C**H$_3$). LC–MS (ESI+): *m/z* calcd for $C_{23}H_{34}N_3O_7$ $[M+H]^+$: 464.24, found 464.25 (t_R = 7.5 min). HRMS (ESI+) *m/z* calcd for $C_{23}H_{33}N_3O_7Na$ $[M+Na]^+$: 486.22107, found 486.2207.

***Tandem* Knoevenagel-PEG-acid**: *Tandem* Knoevenagel-PEG-*tert* butyl ester (61 mg, 132 μmol) was dissolved in CH_2Cl_2 (10 mL) and a 4 M solution of HCl in dioxane (10 mL) was added. The reaction mixture was stirred for 3.5 h at RT. After removal of the solvent, this procedure was repeated for 2.5 h. The product (42 mg, 78%) was obtained after preparative RP-HPLC as a yellowish oil. Amide/iminol ratio: 7:3. ^{1}H NMR (600 MHz, $CDCl_3$, 25 °C): 7.93 (d, ^3J = 8.82 Hz, 2H, Ar-**H**, iminol), 7.84 (d, ^3J = 8.22 Hz, 2H, Ar-**H**, amide), 7.81 (d, ^3J = 8.67 Hz, 2H, Ar-**H**, iminol), 7.64 (d, ^3J = 7.78 Hz, 2H, Ar-**H**, amide), 7.49 (s, 1H, N-**H**, amide), 7.34 (s, 1H, N–**H**, iminol), 5.63 (s, 2H, –CN–C**H**=CO–, iminol), 4.05 (s, 2H, –C**H$_2$**–COOH, amide), 4.03 (s, 2H, –C**H$_2$**–COOH, iminol), 3.57 (m, 12H, PEG), 3.47 (s, 2H, –CN–C**H$_2$**–CO, amide), 2.28 (s, 3H, –C**H$_3$**, amide), 2.13 (s, 3H, –C**H$_3$**, iminol). ^{13}C NMR (151 MHz, $CDCl_3$, 25 °C): 172.66 (–N–N–**C**O), 172.50 (–**C**OOH), 172.32 (–**C**OOH), 169.00 (–**C**O–NH), 167.60 (–**C**O–NH), 161.21 (–CN–**CH**=CO–), 159.56 (–**C**N–CH_3), 151.45 (–**C**N–CH_3), 141.99 (–N–**C$_{Ar}$**), 138.17 (–N–**C$_{Ar}$**), 133.97 (–**C$_{Ar}$**–CO–NH), 130.82 (–**C$_{Ar}$**–CO–NH), 129.29 (–**C$_{Ar}$**–C_{Ar}–CO), 128.99 (–**C$_{Ar}$**–C_{Ar}–CO), 122.45 (–**C$_{Ar}$**–C_{Ar}–N) 118.37 (–**C$_{Ar}$**–C_{Ar}–N), 93.48 (**CH**=C–OH), 71.50 (PEG), 71.45 (PEG), 70.13 (PEG), 71.06 (PEG), 70.04 (PEG), 68.82 (–**C**H$_2$–COOH), 43.91 (–**C**H$_2$–CO), 40.68 (PEG), 40.55 (PEG), 17.09 (–**C**H$_3$), 12.59 (–**C**H$_3$). LC–MS (ESI+): *m/z* calcd for $C_{19}H_{26}N_3O_7$ $[M+H]^+$: 408.17, found 408.18 (t_R = 5.2 min). HRMS (ESI+) *m/z* calcd for $C_{19}H_{25}N_3O_7Na$ $[M+Na]^+$: 430.15847, found 430.1577.

***Tandem* Knoevenagel-mTet (14)**: *Tandem* Knoevenagel-PEG-acid (40 mg, 98.2 μmol), 6-methyltetrazine-amine hydrochloride (28 mg, 117.8 μmol), HOAt (20 mg, 147.3 μmol) and DIPEA (25 μL, 147.3 μmol) were dissolved in DMF (1 mL). EDC·HCl (28.2 mg, 147.3 μmol) was added in portions over 5 min. Finally, the reaction mixture was stirred overnight at RT and then directly purified by preparative HPLC. **14** (53 mg, 86%) was obtained as a red solid. LC–MS analysis showed a slow formation of a side product, which is why this product was only analyzed by LC–MS and HRMS. LC–MS (ESI+): *m/z* calcd for $C_{29}H_{35}N_8O_8$ $[M+H]^+$: 591.27, found 591.20 (t_R =

6.8 min). HRMS (ESI+): *m/z* calcd for $C_{29}H_{35}N_8O_8$ $[M+H]^+$: 591.26741, found 591.2670.

BCN-CF (15): BCN-NHS (4.9 mg, 16.7 μmol), H_2N-PEG_2-5(6)-CF (10 mg, 18.4 μmol) and DIPEA (6.1 μL, 35 μmol) were dissolved in dry DMF (0.5 mL) and stirred overnight at RT. The reaction mixture was directly purified by preparative RP-HPLC. **15** (quant.) was obtained as a yellow solid. LC–MS (ESI+): *m/z* calcd for $C_{38}H_{39}N_2O_{10}$ $[M+H]^+$: 683.26, found: 683.26 (t_R = 8.4 min). HRMS (ESI+): *m/z* calcd for $C_{38}H_{39}N_2O_{10}$ $[M+H]^+$: 683.25992, found: 683.2595.

DBCO-CF (16): DBCO-NHS (7.2 mg, 16.7 μmol), H_2N-PEG_2-5(6)-CF (10 mg, 18.4 μmol) and DIPEA (6.1 μL, 35 μmol) were dissolved in dry DMF (0.5 mL) and stirred overnight at RT. The reaction mixture was directly purified by preparative RP-HPLC and **16** (4.2 mg, 31 %) was obtained as a yellow solid with a purity of approx. 90 % (HPLC). LC–MS (ESI+): $C_{48}H_{44}N_3O_{10}$ $[M+H]^+$: 822.30, found: 822.29 (t_R = 4.6 min). HRMS (ESI+): $C_{48}H_{44}N_3O_{10}$ $[M+H]^+$: 822.30212, found: 822.3015.

Biochemical experiments

Expression and purification of MtFGE and DARPin E01: For MtFGE a 60 mL LB pre-culture containing ampicillin was inoculated with *E. coli* BL21 (DE3) containing the vector pET14b-mtFGE-His_6. For the DARPin-construct a kanamycin pre-culture with *E. coli* BL21 (DE3) containing pET24b-DARPinE01-CTPSR-His_6 (see the Supporting Information; sequences) was generated. After overnight incubation at 37 °C and shaking, a 1 L main culture was inoculated by the harvested cells, respectively. The cultures were incubated at 37 °C and 160 rpm until an optical density (OD_{600}) of 0.6 was reached. Afterwards, the cells were cooled to 18 °C, IPTG (200 μM) was added, and the cultures were incubated for 16 h at 18 °C and 150 rpm. Finally, cells were harvested and stored at −20 °C until further use. The pellets were resuspended in PBS (pH 7.4) and EDTA-free protease inhibitor (Complete, Roche) and DNaseI were added. Cells lysis was performed mechanically by French Press (3× 1000 psi). Cell debris was removed by centrifugation (12850 × *g*, 4 °C, 30 min) and filtration (pore size 0.22 μm). The proteins were purified by an chromatography system (ÄKTA Explorer, GE Healthcare) at 4 °C and Ni^{2+}-NTA affinity chromatography (HisTrap HP, 1 mL, GE Healthcare). The sample was loaded and washed with binding buffer (50 mM NaH_2PO_4, 300 mM NaCl, 25 mM imidazol, pH 8.0) and then eluted using a linear imidazole gradient (25-250 mM). The isolated enzyme, tested by SDS-Gel, was pooled and rebuffered in PBS (pH 7.4) using Vivaspin centrifugal concentrators (MWCO 5000, Sartorius). For MtFGE and DARPin, an average of 30–40 mg was obtained per 1 L of cell culture. The enzyme was either used immediately or stored in the presence of 200 mM arginine and the DARPin with 20 mM arginine at −80 °C until further use.

SDS-polyacrylamide gel electrophoresis (SDS-PAGE) was performed using 10, 12.5 or 15 % acrylamide in the running gel and 5 % in the stacking gel. Bisacrylamide was used as crosslinker. Protein samples were incubated either for 5 min at 95 °C or for 1 h at 37 °C with 4x Laemmli buffer plus 20 % 2-mercaptoethanol. Separation was obtained overnight with 4 mA or in 3 h with 30 mA. After completion, the gel was washed with water for 5 min and then treated with staining solution (50 % MeOH, 10 % AcOH, 40 % H_2O, 0.1 % Coomassie Brilliant Blue) for 3 h. Destaining was performed after several washing steps with 40 % MeOH, 10 % AcOH and 40 % H_2O, followed by documentation with a CCD camera (Fujifilm).

Protein concentrations were determined by Bradford assay with Coomassie brilliant blue G-250 (200 μL) and a BSA standard. All samples were measured in duplicates.

Enzymatic conversion of DARPin E01 with MtFGE: DARPin-E01 with CTPSR-motif (574 μL in PBS buffer containing 20 mM arginine, 7.63 mg/mL) was diluted with bicine buffer (800 μL, 150 mM bicine, 200 mM NaCl, 600 mM arginine), water (721 μL) and 100 mM DTT (120 μL) and subsequently incubated with MtFGE (180 μL in PBS + 20 mM arginine, 5 mg/mL, final concentration 10 μM), 10 mM $CuSO_4$ (2.4 μL, final concentration 10 μM) and 10 mM $CaCl_2$ (2.4 μL, final concentration 10 μM) for 16–20 h at 22–25 °C. The reaction progress was monitored by tryptic digest (4 h at 37 °C) and MALDI-ToF-MS (UltrafleXtreme, Bruker Daltonics). Precipitated MtFGE was centrifuged and the FGly-containing DARPin rebuffered into either HIPS (100 mM phosphate, 20 mM NaCl, pH 6.0) or Knoevenagel ligation buffer (50 mM citrate, 50 mM NaCl, pH 7.2) using size exclusion desalting with a PD10 (GE) column.

Time- and equivalent-dependent fluorescent labeling of FGly-containing DARPin E01: 30 μM of FGly-containing DARPin E01 in HIPS or Knoevenagel buffer was treated for 24 h at 22 °C with 2.5, 5, 7.5 and 10 equiv. of HIPS-CF (**2**) or *trapped* Knoevenagel-CF (**9**). Samples (15 μg of protein) were taken after 2, 6, 10 and 24 h and stored at −80 °C until they were analyzed by SDS-PAGE (15 %). Therefore, the samples were diluted with 4xLaemmli buffer (containing 20 % 2-mercaptoethanol) and incubated for 5 min at 95 °C.

Preparative fluorescent labeling via *trapped* Knoevenagel: For complete labeling via standard Knoevenagel chemistry, 100 μM of the previously obtained FGly-containing DARPin was incubated for 24 h at 22 °C with 1 mM of *trapped* Knoevenagel-CF (**9**). Afterwards, DARPin-CF was rebuffered into PBS (pH 7.4) using PD10 and stored at −80 °C until further use.

Conversion of FGly-DARPin with azides 6 and 12: The obtained FGly-containing DARPins were directly treated either with 2 mM of **6** for 16 h at 30 °C or with 10 mM of **12** for 24 h at 22 °C. Afterwards, DARPin-N_3 (generated using **6**) and DARPin-$(N_3)_2$ (generated using **12**) were rebuffered into a phosphate buffer (8 % DMSO, 100 mM phosphate, 150 mM NaCl, pH 7.2) and stored at −80 until further use.

Stability assay with HIPS-azide (6): HIPS-azide (**6**) was diluted under aerobic conditions in HIPS ligation buffer (final concentration of 2 mM) and different additives (1 mM EDTA, 0.1 mM CuI, 0.1 mM $CuSO_4$) were added. Additionally, HIPS-azide (6) was incubated without additives under aerobic and anaerobic conditions. The samples were incubated for 16 h at 30 °C and subsequently analyzed via LC–MS.

Click-reaction with different strained alkynes: DARPin-N_3 and DARPin-$(N_3)_2$ were treated with different equivalents of DBCO-CF (**16**) for 4 h at 22 °C, BCN-CF (**15**) for 16 h at 22 °C or DBCO-PEG_{20k} (**17**) for 16 h at 37 °C. Afterwards, the reactions were directly analyzed by SDS-PAGE. Samples were diluted with 4xLaemmli buffer (containing 20 % 2-mercaptoethanol) and incubated for 1 h at 37 °C.

For selective PEG-staining, the colored/non-colored gel was washed with water (3x5 min), incubated for 10 min with a 5 % $BaCl_2$ solution, washed again with water (3x2 min) and finally incubated for 5 min with 0.1 % iodine solution.

For preparative scale, the DARPin-CF_2, generated by **12** and **16**, was rebuffered into PBS (pH 7.4) using PD10 and stored at −80 °C until further use.

Live-cell imaging: A431 and MCF7 cell lines were cultivated in μ-Slides 8 Well (ibidi GmbH) with $2.5 \cdot 10^4$ cells per 1.0 cm^2 surface area (37 °C, 5 % CO_2 atmosphere). Cells were washed with RPMI medium once before and twice after incubation with 100 nM DARPin conjugates (in PBS, pH 7.4) for 6–8 h either at 4 °C or 37 °C.

5% CO_2 atmosphere was not maintained at 4 °C. LysoTracker DND-22 was added to a final concentration of 150 nM to cells incubated at 37 °C. Imaging was performed with the confocal fluorescence microscope Zeiss LSM 780 using the objective LCI Plan-Neofluar 63x/1.3 Imm Corr DIC M27. The line sequential scanning mode for the green (λ_{ex} = 488 nm, λ_{em} = 499–553 nm) and blue (λ_{ex} = 405 nm, λ_{em} = 415–466 nm) channel was used to minimize the effect of lysosomal movement for colocalization analysis. The argon ion laser was run with 2.0% laser power to excite CF. The green fluorescence was detected by the 32-ch GaAsp detector (gain 700, detector offset 0 digital gain 1.0). 12-bit images were processed with the ImageJ software: equal brightness adjustment for green channels (3-345), rescaling to 16-bit images, analysis of mean fluorescence intensity, individual thresholding for both channels for pseudo-coloring of overlaying pixels.

Acknowledgements

This work was supported by Deutsche Forschungsgemeinschaft as part of the priority program SPP 1623 (DI 575/9-1, MU 2286/6-1, SE 609/15-1). The pET14b-mtFGE-His$_6$ plasmid was provided by David Rabuka (Redwood Bioscience, Emeryville, USA). Open access funding enabled and organized by Projekt DEAL.

Conflict of Interest

The authors declare no conflict of interest.

Keywords: bioconjugation · branched PEG linker · click chemistry · formylglycine · HIPS ligation · Knoevenagel ligation

[1] C. D. Spicer, B. G. Davis, *Nat. Commun.* **2014**, *5*, 1–14.
[2] A. Borrmann, J. C. M. Van Hest, *Chem. Sci.* **2014**, *5*, 2123–2134.
[3] E. M. Sletten, C. R. Bertozzi, *Angew. Chem. Int. Ed.* **2009**, *48*, 6974–6998; *Angew. Chem.* **2009**, *121*, 7108–7133.
[4] P. Shieh, C. R. Bertozzi, *Org. Biomol. Chem.* **2014**, *12*, 9307–9320.
[5] J. E. Hudak, R. M. Barfield, G. W. Dehart, P. Grob, E. Nogales, C. R. Bertozzi, D. Rabuka, *Angew. Chem. Int. Ed.* **2012**, *51*, 4161–4165; *Angew. Chem.* **2012**, *124*, 4237–4241.
[6] S. Bloess, T. Beuel, T. Krüger, N. Sewald, T. Dierks, G. Fischer von Mollard, *Appl. Microbiol. Biotechnol.* **2019**, *103*, 2229–2241.
[7] P. M. Drake, A. E. Albers, J. Baker, S. Banas, R. M. Barfield, A. S. Bhat, G. W. De Hart, A. W. Garofalo, P. Holder, L. C. Jones, et al., *Bioconjugate Chem.* **2014**, *25*, 1331–1341.
[8] R. Kudirka, R. M. Barfield, J. McFarland, A. E. Albers, G. W. De Hart, P. M. Drake, P. G. Holder, S. Banas, L. C. Jones, A. W. Garofalo, et al., *Chem. Biol.* **2015**, *22*, 293–298.
[9] Q. Wang, A. R. Parrish, L. Wang, *Chem. Biol.* **2009**, *16*, 323–336.
[10] H. Neumann, *FEBS Lett.* **2012**, *586*, 2057–2064.
[11] K. Strijbis, E. Spooner, H. L. Ploegh, *Traffic* **2012**, *13*, 780–789.
[12] R. R. Beerli, T. Hell, A. S. Merkel, U. Grawunder, *PLoS One* **2015**, *10*, 1–17.
[13] M. W. L. Popp, H. L. Ploegh, *Angew. Chem. Int. Ed.* **2011**, *50*, 5024–5032; *Angew. Chem.* **2011**, *123*, 5128–5137.
[14] P. R. Spycher, C. A. Amann, J. E. Wehrmüller, D. R. Hurwitz, O. Kreis, D. Messmer, A. Ritler, A. Küchler, A. Blanc, M. Béhé, et al., *ChemBioChem* **2017**, *18*, 1923–1927.
[15] P. Dennler, A. Chiotellis, E. Fischer, D. Brégeon, C. Belmant, L. Gauthier, F. Lhospice, F. Romagne, R. Schibli, *Bioconjugate Chem.* **2014**, *25*, 569–578.
[16] V. Siegmund, S. Schmelz, S. Dickgiesser, J. Beck, A. Ebenig, H. Fittler, H. Frauendorf, B. Piater, U. A. K. Betz, O. Avrutina, et al., *Angew. Chem. Int. Ed.* **2015**, *54*, 13420–13424; *Angew. Chem.* **2015**, *127*, 13618–13623.
[17] H. Schneider, L. Deweid, O. Avrutina, H. Kolmar, *Anal. Biochem.* **2020**, *595*, 113615.
[18] M. Rashidian, S. C. Kumarapperuma, K. Gabrielse, A. Fegan, C. R. Wagner, M. D. Distefano, *J. Am. Chem. Soc.* **2013**, *135*, 16388–16396.
[19] K. F. Geoghegan, J. G. Stroh, *Bioconjugate Chem.* **1992**, *3*, 138–146.
[20] J. M. Gilmore, R. A. Scheck, A. P. Esser-Kahn, N. S. Joshi, M. B. Francis, *Angew. Chem. Int. Ed.* **2006**, *45*, 5307–5311; *Angew. Chem.* **2006**, *118*, 5433–5437.
[21] J. Landgrebe, T. Dierks, B. Schmidt, K. Von Figura, *Gene* **2003**, *316*, 47–56.
[22] J. Peng, S. Alam, K. Radhakrishnan, M. Mariappan, M. G. Rudolph, C. May, T. Dierks, K. Von Figura, B. Schmidt, *FEBS J.* **2015**, *282*, 3262–3274.
[23] K. Von Figura, B. Schmidt, T. Selmer, T. Dierks, *BioEssays* **1998**, *20*, 505–510.
[24] M. Knop, T. Q. Dang, G. Jeschke, F. P. Seebeck, *ChemBioChem* **2017**, *18*, 161–165.
[25] P. G. Holder, L. C. Jones, P. M. Drake, R. M. Barfield, S. Bañas, G. W. De Hart, J. Baker, D. Rabuka, *J. Biol. Chem.* **2015**, *290*, 15730–15745.
[26] T. Dierks, B. Schmidt, L. V. Borissenko, J. Peng, A. Preusser, M. Mariappan, K. Von Figura, *Cell* **2003**, *113*, 435–444.
[27] T. Dierks, *EMBO J.* **1999**, *18*, 2084–2091.
[28] T. Krüger, S. Weiland, G. Falck, M. Gerlach, M. Boschanski, S. Alam, K. M. Müller, T. Dierks, N. Sewald, *Angew. Chem. Int. Ed.* **2018**, *57*, 7245–7249; *Angew. Chem.* **2018**, *130*, 7365–7369.
[29] R. J. Spears, M. A. Fascione, *Org. Biomol. Chem.* **2016**, *14*, 7622–7638.
[30] P. Agarwal, C. R. Bertozzi, *Bioconjugate Chem.* **2015**, *26*, 176–192.
[31] A. Dirksen, P. E. Dawson, *Bioconjugate Chem.* **2008**, *19*, 2543–2548.
[32] A. Dirksen, T. M. Hackeng, P. E. Dawson, *Angew. Chem. Int. Ed.* **2006**, *45*, 7581–7584; *Angew. Chem.* **2006**, *118*, 7743–7746.
[33] B. M. Mueller, W. A. Wrasidlo, R. A. Reisfeld, *Bioconjugate Chem.* **1990**, *1*, 325–330.
[34] I. S. Carrico, B. L. Carlson, C. R. Bertozzi, *Nat. Chem. Biol.* **2007**, *3*, 321–322.
[35] M. A. Frese, T. Dierks, *ChemBioChem* **2009**, *10*, 425–427.
[36] J. Kalia, R. T. Raines, *Angew. Chem. Int. Ed.* **2008**, *47*, 7523–7526; *Angew. Chem.* **2008**, *120*, 7633–7636.
[37] T. Sasaki, K. Kodama, H. Suzuki, S. Fukuzawa, K. Tachibana, *Bioorg. Med. Chem. Lett.* **2008**, *18*, 4550–4553.
[38] P. Agarwal, J. Van Der Weijden, E. M. Sletten, D. Rabuka, C. R. Bertozzi, *Proc. Natl. Acad. Sci. USA* **2013**, *110*, 46–51.
[39] P. Agarwal, R. Kudirka, A. E. Albers, R. M. Barfield, G. W. De Hart, P. M. Drake, L. C. Jones, D. Rabuka, *Bioconjugate Chem.* **2013**, *24*, 846–851.
[40] S. Pomplun, M. Y. H. Mohamed, T. Oelschlaegel, C. Wellner, F. Bergmann, *Angew. Chem. Int. Ed.* **2019**, *58*, 3542–3547.
[41] M. J. Han, D. C. Xiong, X. S. Ye, *Chem. Commun.* **2012**, *48*, 11079–11081.
[42] J. Alam, T. H. Keller, T. P. Loh, *J. Am. Chem. Soc.* **2010**, *132*, 9546–9548.
[43] P. Wang, S. Zhang, Q. Meng, Y. Liu, L. Shang, Z. Yin, *Org. Lett.* **2015**, *17*, 1361–1364.
[44] R. A. Kudirka, R. M. Barfield, J. M. McFarland, P. M. Drake, A. Carlson, S. Banas, W. Zmolek, A. W. Garofalo, D. Rabuka, *ACS Med. Chem. Lett.* **2016**, *7*, 994–998.
[45] J. Yu, D. Shen, H. Zhang, Z. Yin, *Bioconjugate Chem.* **2018**, *29*, 1016–1020.
[46] B. Spangler, S. Yang, C. M. Baxter Rath, F. Reck, B. Y. Feng, *ACS Chem. Biol.* **2019**, *14*, 725–734.
[47] R. Walder, M. A. Leblanc, W. J. Van Patten, D. T. Edwards, J. A. Greenberg, A. Adhikari, S. R. Okoniewski, R. M. A. Sullan, D. Rabuka, M. C. Sousa, et al., *J. Am. Chem. Soc.* **2017**, *139*, 9867–9875.
[48] M. F. Debets, S. S. Van Berkel, S. Schoffelen, F. P. J. T. Rutjes, J. C. M. Van Hest, F. L. Van Delft, *Chem. Commun.* **2010**, *46*, 97–99.
[49] B. L. Oliveira, Z. Guo, G. J. L. Bernardes, *Chem. Soc. Rev.* **2017**, *46*, 4895–4950.
[50] S. Goswami, H. S. Jena, S. Konar, *Inorg. Chem.* **2014**, *53*, 7071–7073.
[51] S. G. Tolshchina, G. L. Rusinov, V. N. Charushin, *Chem. Heterocycl. Compd.* **2013**, *49*, 66–91.
[52] A. L. Handlon, N. J. Oppenheimer, *Pharm. Res.* **1998**, 5, 297–299.
[53] R. Van Geel, G. J. M. Pruijn, F. L. Van Delft, W. C. Boelens, *Bioconjugate Chem.* **2012**, *23*, 392–398.
[54] C. Zhang, P. Dai, A. A. Vinogradov, Z. P. Gates, B. L. Pentelute, *Angew. Chem. Int. Ed.* **2018**, *57*, 6459–6463; *Angew. Chem.* **2018**, *130*, 6569–6573.
[55] S. Samanta, S. Ray, A. B. Ghosh, P. Biswas, *RSC Adv.* **2016**, *6*, 39356–39363.
[56] K. Renault, C. Guillou, P. Y. Renard, C. Sabot, *Org. Biomol. Chem.* **2019**, *17*, 388–396.

[57] D. Steiner, P. Forrer, A. Plückthun, *J. Mol. Biol.* **2008**, *382*, 1211–1227.
[58] S. Zhang, L. M. De Leon Rodriguez, I. K. H. Leung, G. M. Cook, P. W. R. Harris, M. A. Brimble, *Angew. Chem. Int. Ed.* **2018**, *57*, 3631–3635; *Angew. Chem.* **2018**, *130*, 3693–3697.
[59] Z. J. Liu, S. Martínez Cuesta, P. van Delft, S. Balasubramanian, *Nat. Chem.* **2019**, *11*, 629–637.
[60] T. Linz, D. Yeo, Q. Hong, W. Zmolek, J. McFarland, R. Barfield, W. Haskins, D. Rabuka, *Antibodies* **2018**, *7*, 40.
[61] Y. Anami, C. M. Yamazaki, W. Xiong, X. Gui, N. Zhang, Z. An, K. Tsuchikama, *Nat. Commun.* **2018**, *9*, 1–9.
[62] J. Dommerholt, O. Van Rooijen, A. Borrmann, C. F. Guerra, F. M. Bickelhaupt, F. L. Van Delft, *Nat. Commun.* **2014**, *5*, 1–7.
[63] M. M. Kurfürst, *Anal. Biochem.* **1992**, *200*, 244–248.
[64] A. Moosmann, E. Müller, H. Böttinger, *Methods Mol. Biol. Protein Downstr. Process. Des. Dev. Appl. High Low-Resolution Methods* **2014**, *1129*, 572–538.
[65] F. Selis, G. Focà, A. Sandomenico, C. Marra, C. Di Mauro, G. S. Jotti, S. Scaramuzza, A. Politano, R. Sanna, M. Ruvo, et al., *Int. J. Mol. Sci.* **2016**, *17*, 1–15.
[66] R. C. Feiner, I. Pennè, B. Müller, K. M. Müller, *Biochemistry* **2019**, *58*, 1043–1047.
[67] R. B. Dickson, J. A. Hanover, M. C. Willingham, I. Pastan, *Biochemistry* **1983**, *22*, 5667–5674.

Manuscript received: June 29, 2020
Revised manuscript received: August 5, 2020
Accepted manuscript online: August 6, 2020
Version of record online: September 18, 2020